Geoenvironmental Disasters

REVIEW

Open Access

Failure mechanism, existing constitutive models and numerical modeling of landslides in sensitive clay: a review

Zinan Ara Urmi[1*], Ali Saeidi[1], Rama Vara Prasad Chavali[1] and Alba Yerro[2]

Abstract

Landslides involving sensitive clays are recurrent events in the world's northern regions and are especially notorious in eastern Canada. The two critical factors that separate sensitive clay landslides from traditional slope stability analysis are the highly brittle behavior in undrained conditions (strain-softening) characteristic of progressive or retrogressive failures and the large deformations associated with them. Conventional limit equilibrium analysis has numerous shortcomings in incorporating these characteristics when assessing landslides in sensitive clays. This paper presents an extensive literature review of the failure mechanics characteristics of landslides in sensitive clays and the existing constitutive models and numerical tools to analyze such slopes' stability and post-failure behavior. The advantages and shortcomings of the different techniques to incorporate strain-softening and large deformation in the numerical modeling of sensitive clay landslides are assessed. The literature review depicts that elastoviscoplastic soil models with non-linear strain-softening laws and rate effects represent the material behavior of sensitive clays. Though several numerical models have been proposed to analyze post-failure runouts, the amount of work performed in line with sensitive clay landslides is very scarce. That creates an urgent need to apply and further develop advanced numerical tools for better understanding and predicting these catastrophic events.

Keywords Progressive landslide, Sensitive clay, Numerical modeling, Strain-softening, Constitutive soil model, Large deformation

Introduction

Landslides in sensitive clays are recurrent events in the northern countries of the world, especially in Canada and Norway. The impact of landslides is catastrophic to both the population and the economy. Natural resources Canada (NRCan) has reported that in Canada, the annual damages by landslides are worth $200 to $400 million (NRCan 2019). A total of 778 people have died in landslide events all over the country from 1771 to 2018, among which 134 fatalities are recorded solely in the Québec region due to the glaciomarine-sensitive clay failures in the St. Lawrence Lowlands (Blais-Stevens 2019). Because of the nature of sensitive clay, the runout and affected area of these landslides are generally very large. In the sensitive clays of Norway, the Gjerdrum landslide (2020) spanned a flow-off area of 210,000 m^2 and additionally affected 90,000 m^2 by debris flow. A total of 1000 people were evacuated, ten people died, 31 houses were destroyed, and the mitigation works were worth $20 million without the rebuilding cost of infrastructure or environmental damages (Liu et al. 2021). Therefore, understanding the triggering factors, failure mechanisms, and post-failure consequences of these landslides is vital for risk assessment and improving the resiliency of the affected communities.

*Correspondence:
Zinan Ara Urmi
zaurmi@etu.uqac.ca
[1] Université du Québec à Chicoutimi, 555 Bd de L'Université, Chicoutimi, Saguenay, QC G7H 2B1, Canada
[2] Virginia Tech, Blacksburg, VA 24061, USA

Understanding how material sensitivity controls soil behavior is of utmost importance in analyzing landslides in sensitive clays. The unique nature of sensitive clays is that under shear loading, after reaching the peak shear strength, there is a dramatic reduction in shear strength with increasing strain (Pusch 1966); this phenomenon is generally referred to as "strain-softening." In this context, "sensitivity" is defined as the ratio of the peak shear strength to the reduced shear strength that expresses the loss of strength when the soil experiences large deformation (Crawford 1968; Skempton and Northey 1952). The development of sensitivity of the clays is attributed to the depositional features of sensitive clays as well as the ongoing weathering effect on embankment soils. Sensitive clays are believed to be deposited in marine environment depressions left by the Laurentian ice sheet around 14,000 to 6000 years ago from the present time (Quigley 1980; Lefebvre 1996, 2017). Due to the exposure to seawater with high salt concentration, the clays formed a flocculated structure with high undisturbed shear strength. With the deglaciation of the ice sheets over time, the lands which were once depressed by the huge weight of the ice sheets rose above the sea level (iso-static rebound). Due to this uplift of the clay deposition above the seawater, the clays got exposed to fresh water. When the freshwater flows through the soil, the salt concentration within the soil mass reduces due to the leaching out of salt into the fresh water. As a result, even though the clays retain their flocculated structure, they do not have the salt ions that were keeping the structure stable. This structure is called meta-stable, which is highly susceptible to disturbance and leads to very low remolded strength. Some marine clay deposits exhibit exceptionally high sensitivity after the significant reduction in shear strength with increasing strain; the soil completely loses its structural stability and transforms from a solid to a liquid-like substance (Rosenqvist 1953, 1966). This process is termed "remolding of sensitive clays," and the shear strength at which the process of remolding begins is termed the "remolded shear strength." These soil deposits are also referred to as "quick clays." Sensitivity values for quick clays are generally greater than 30 with remolded shear strength less than 0.5 kPa (Lefebvre 1996). Crawford (1968) reported that eastern Canadian quick clays have a sensitivity value ranging from 20 to several hundred. In a sensitive clay landslide, the initially deformed soil deposits get remolded and flow away from the source area, leaving the newly formed slope unsupported, which may initiate another instability. This process can lead to a series of failures extending far beyond the crest of the initial slope (Bjrrum 1955). Hence, for highly sensitive clays, the slope failure initiation is not the only concern, but the post-failure analysis is also critical. The subsequent sliding is referred to as "progressive" if the failure progresses forward and "retrogressive" if the failure propagates rearward (Varnes 1978).

The current state of knowledge related to the detailed analysis of landslides in sensitive clays depicts that computational modeling is more adaptable than other approaches, such as theoretical analysis, empirical analysis, and experimental investigations. Conventional limit equilibrium analysis has numerous shortcomings in incorporating complex geometry, non-linear soil behavior, and real-life field condition. Moreover, it cannot predict post-failure runout. Alternatively, numerical modeling is a handy tool for slope stability analysis because it requires fewer assumptions, especially regarding the failure mechanism, and can account for complex constitutive behaviors. Even though numerical modeling for landslides has come a long way in the last three decades, a few works have focused on the challenging features of sensitive clays (e.g., strain-softening, the transition from solid to liquid form, and post-failure large deformation) (Dey et al. 2015; Tran and Sołowski 2019; Wang et al. 2022). The reasons for this lack of information are, for example, that the simulation of strain-softening materials is challenging in continuum numerical frameworks, strains tend to develop and localize along narrow shear bands, and several mesh-regularization techniques need to be adapted to obtain mesh-independent results (Rødvand et al. 2022; Singh et al. 2021; Thakur 2011). In addition, a well-established constitutive framework is required to capture the transition from solid to liquid behavior. Finally, the modeling of post-failure behavior in history-dependent materials is complex, and current state-of-practice numerical techniques (i.e., finite elements and finite differences) suffer from mesh tangling when dealing with large deformations (Sulsky et al. 1994).

The objective of this paper is to provide an extensive review of (a) the behavior of sensitive clays under shear loading, (b) the landslide mechanisms in sensitive clays, and (c) the available numerical models (i.e., constitutive laws and numerical frameworks) used for the assessment of such landslides by examining the concerns and advancements of each technique. The paper is organized as follows. First, the post-peak stress–strain behavior of sensitive clays is presented. Then, typical sensitive clay landslides' triggering and failure mechanisms (i.e., flows and spreads) are outlined. After that, the existing numerical tools used for the evaluation of sensitive clay landslides are revised. In particular, the specific utility of constitutive models that address strain-softening and numerical frameworks that cover large deformation problems in the assessment of landslides are discussed. Finally, the literature review is compiled in a summary

table, and the conclusions and future research lines are highlighted.

Behavior of sensitive clays

When subjected to monotonic shear loading in drained conditions, sensitive clays have a robust collapsible nature for both normally consolidated (NC) or over consolidated (OC) state. Due to the depositional history of sensitive clays, during drained shear failure, they experience a dispersion in their meta-stable structure and a simultaneous decrease in porosity (Enyang et al. 2019). In contrast, the non-sensitive clays show dilative or contractive nature in drained shearing based on being OC or NC, respectively. This difference in volumetric behavior in drained conditions directly impacts the undrained behavior of clays. Although no volumetric deformation is expected in undrained conditions, the material's tendency to contract or dilate governs the sign of the excess pore pressure (positive or negative, respectively) generated during the loading process, impacting the undrained shear strength and the soil behavior. While non-sensitive OC clays generate negative pore pressure (suction) and experience enhanced undrained shear strength (with respect to the drained condition), non-sensitive NC clays generate (positive) excess pore water pressures leading to reduced undrained shear strength. Mild strain-softening behavior might be observed in either case, but it does not greatly impact shearing resistance. On the contrary, in sensitive clays (NC or OC), the strong tendency to collapse leads to a massive generation of excess pore pressure, the shearing resistance is reduced to a negligible value, and the strain-softening behavior is exacerbated in comparison with the one experienced by non-sensitive clays (Lefebvre 1981). Both non-sensitive and sensitive OC clays exhibit similar strain-softening behavior in drained conditions.

Early studies on the stress–strain behavior of sensitive clays explicated strain-softening phenomenon based on experimental results (Skempton 1964; Skempton and Northey 1952). Skempton (1964) illustrated that if overconsolidated clays are strained, the shear strength would initially increase up to a certain point (peak shear strength). Then, the strength would start to decrease gradually with increasing strain to a residual value at a large displacement. He stipulated that post-peak strain-softening occurs due to the reduction of the effective cohesion (c') and friction angle (ϕ') of such clays to a residual value (c'_r and ϕ'_r) (Fig. 1). Bjrrum (1961) suggested that in undrained shearing, increasing pore pressure with increasing strain might cause a decrease in shearing resistance due to the diminished effective stress. Consistent with this idea, several researchers in the last two decades stipulated that the post-peak shear strength reduction in soft sensitive clays is governed by shear-induced pore pressure rather than by a reduction of the values of the strength parameters (ϕ' and c′) (Bernander 2000; Gylland et al. 2012; Thakur 2011, 2007; Thakur et al. 2006). Figure 2 represents the stress–strain relationship and stress paths of CU triaxial testing, where the undrained effective stress path (ESP) follows a unique failure line when subjected to undrained shearing (Thakur et al. 2014). The resulting undrained strain-softening behavior is related to the increasing shear-induced pore pressure (P_w), thereby reducing the effective stress. Thakur et al. (2014) supported that reductions in ϕ' and c′ are possible when sensitive clays are subjected to very large strains, which was demonstrated in constant volume ring shear test results on low-sensitive Drammen plastic clay (Stark and Eid 1994).

Canadian sensitive clays can have a remolded undrained shear strength s_{ur} less than 1.5 kPa measured by Swedish fall cone tests (Demers et al. 2014; Locat et al.

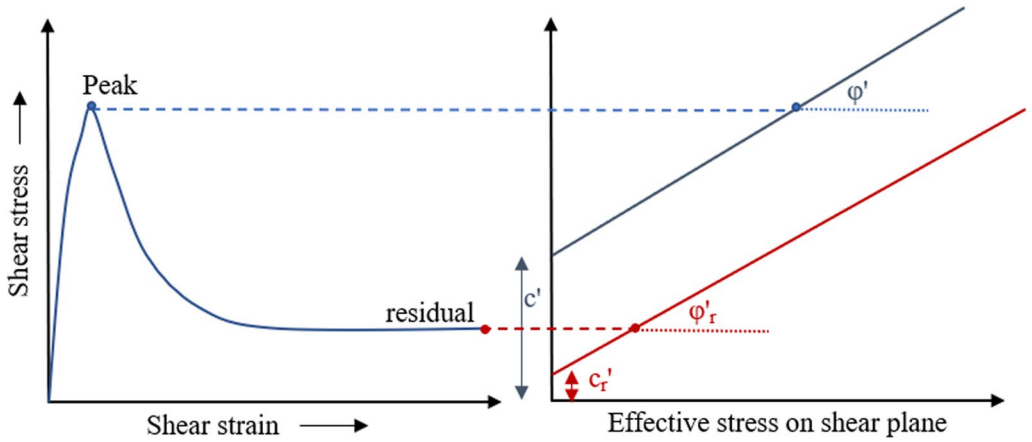

Fig. 1 Drained behavior of an overconsolidated clay under shear loading (after Skempton 1964)

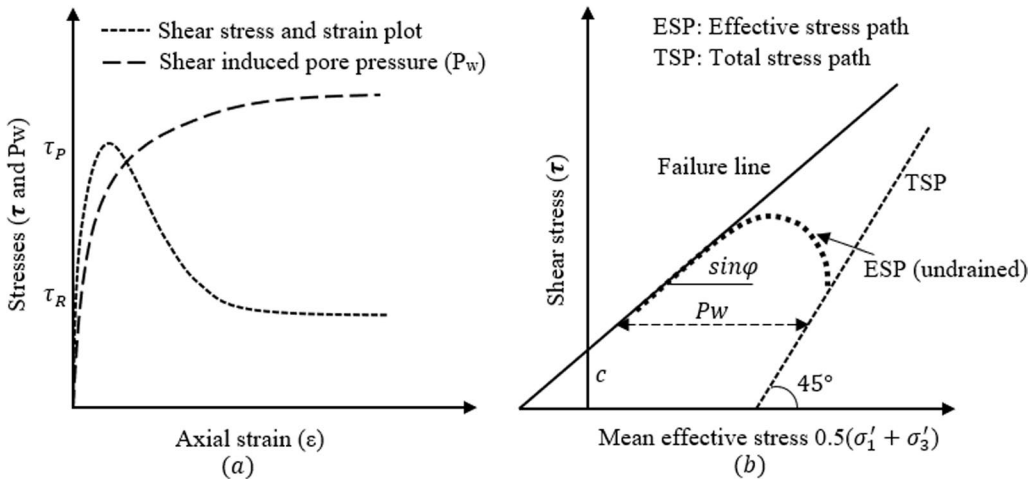

Fig. 2 Illustration of the strain-softening mechanism. **a** Development of excess pore water pressure resulting in reduced shear strength; and **b** Effective stress path and total stress path following a unique failure line indicating no reduction in effective cohesion and friction angle (after Thakur et al. 2014)

2017, 2015). Tavenas et al. (1983) determined the strain energy required to remold sensitive clays up to a certain percentage (75–90%) for different locations in eastern Canada and plotted the remolding index (I_r) vs. strain energy curves. Later on, Quinn et al. (2011) converted those curves to stress–strain curves and pointed out that the shear strain required for 75%-90% of remolding is far beyond 100% (Fig. 3a). Stark and Contreras (1996) also suggested that a wholly remolded state may occur when the specimen is sheared to several hundred millimeters, equivalent to several hundred percent shear strain in soil specimens subjected to conventional laboratory tests. But such large strains cannot be attained by standard laboratory shear testing. Stress–strain curves obtained from triaxial compression tests are limited to only 10–20% strain (Thakur et al. 2014). Generally, ring shear tests, reversal shear box tests, or direct simple shear tests are used to study the large deformation behavior, but these laboratory-scale shear tests could only achieve strains up to 30–45% (Durand 2016; Locat 2007; Locat et al. 2017, 2015, 2013). This limitation warrants the need for strain-softening equations to predict the complete post-peak softening behavior up to the remolded stress (Urmi et al. 2022). Figure 3b illustrates DSS results in undrained conditions for sensitive clays from five different locations in Canada; it can be observed that strain-softening in sensitive clays is highly non-linear.

The behavior of sensitive clays is significantly affected by the deformation rate. Vaid et al. (1979) performed one-dimensional and isotropic consolidation triaxial tests on heavily consolidated sensitive clay. They observed that the compressibility and the undrained shear strength considerably depend on the development of time-dependent strain, generally known as creep. Creep is a phenomenon in which a soil mass undergoes a slow and gradual deformation over time while subjected to constant effective stress (Yin et al. 2011). It was noted that low strain rates caused increased compressibility and reduced shear strength. Other studies on sensitive Leda clay also support the fact that the undrained shear strength of the soil increased by about 6–12% for a ten times increase in strain rate (Graham et al. 1983; Leroueil et al. 1985). Lefebvre and Leboeuf (1987) found a linear variation of shear strength with the logarithm of strain rate by performing several monotonic and cyclic triaxial tests on three undisturbed sensitive clay samples from eastern Canada (Fig. 4).

Field observations of sensitive clay landslides have indicated that the creep behavior significantly influences the field conditions for landslide initiation in glacimarine-sensitive clays (Okamoto et al. 2004). Creep development leading to failure has three stages, a primary stage when the strain rate decreases over time, a secondary stage where the strain rate is constant, and a tertiary phase when the change in strain rate accelerates until global failure occurs (Okamoto et al. 2004; Yin et al. 2011). Neglecting the impact of strain rate during the primary stage can promote the initiation of failure. However, during the tertiary phase, not considering strain rate can lead to overestimating the velocity of flowing debris, resulting in more significant retrogression and runout.

In sensitive clays, the sliding surface may develop in a narrow shear band due to the strain-softening response before any significant movement occurs. The strength degradation process is initiated when the gravitational shear stress surpasses the peak strength. As a result,

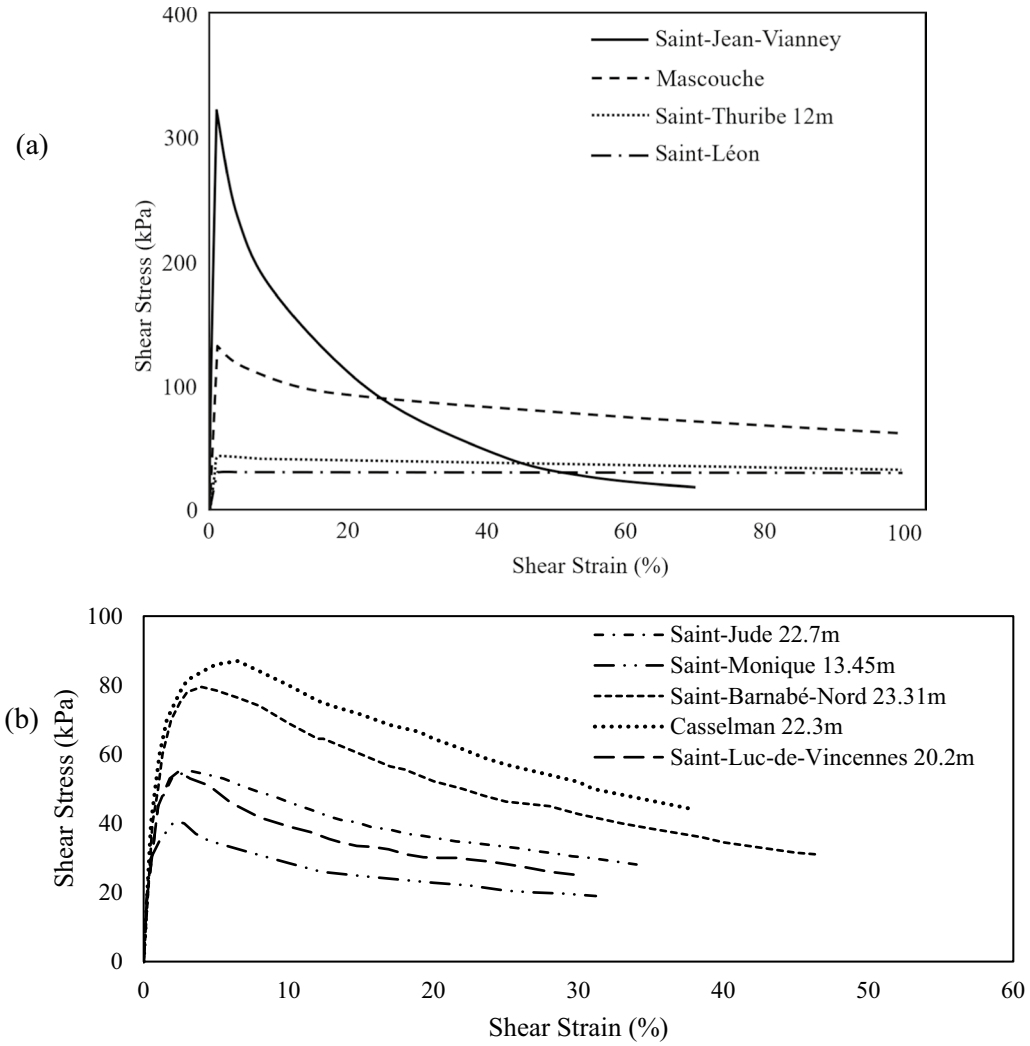

Fig. 3 **a** Analytically interpreted stress–strain curves based on the data of the remolding index vs. normalized strain energy curves by Tavenas et al. (1983) (after Quinn et al. 2011) **b** Experimental DSS test results showing strain-softening behavior of sensitive clays for different locations in Canada; the legends show the depth of the sample along with the location name (after Durand 2016; Locat 2007; Locat et al. 2017, 2015, 2013)

unbalanced stresses are transferred to the surrounding areas, potentially overstressing the neighboring points. This process eventually leads to the development of a continuous weak zone where all the subsequent plastic deformation occurs, generally known as a shear band (Zhang and Wang 2020). The energy released during strain softening acts as the driving force for the propagation of the shear band. The shear band propagates steadily as long as the mobilized strength within the shear band is lower than the peak strength but greater than the remolded strength. When plastic deformations further reduce the shear strength in the weak zone to the remolded strength, the shear band can progressively propagate without additional external load (Quinn et al. 2011). The required length for the catastrophic propagation of the shear band is known as the characteristic length or the critical length of the shear band. Several analytical and numerical methods exist to evaluate this critical length (Puzrin and Germanovich 2005; Quinn et al. 2012; Zhang et al. 2015). Propagation of shear bands beyond their critical length leads to large retrogressive failures in sensitive clays. Detailed descriptions of the formation of the sliding surface in sensitive clay landslides can be found in Locat et al.'s (2011) work.

Landslide types and failure mechanisms

Sensitive clays (quick clays) are postglacial marine deposits found primarily in North America (Eastern Canada and Alaska) and Scandinavia (Torrance 1983). The largest deposits of postglacial marine clays

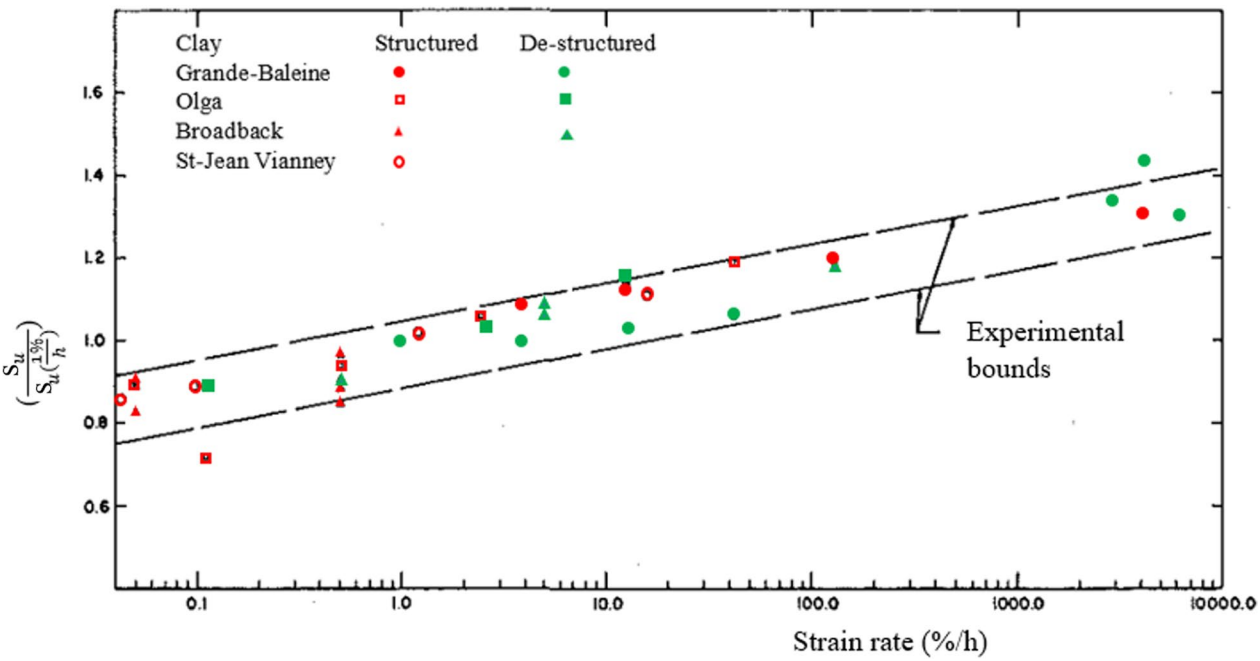

Fig. 4 Change in undrained shear strength ratio with strain rate (after Lefebvre and LeBoeuf 1987)

were formed in the Champlain Sea in the Saint-Lawrence lowland, approximately 12,500 to 10,000 years BP (Hillaire-Marcel 1980). Lefebvre (1986) identified landslides as an important feature of valley formation caused by erosion of rivers and streams. He emphasized that the erodibility of the clay layers and change in groundwater regime in these deposits are major causes of instability. Demers et al. (2014) illustrated that the majority of the landslides in Canadian sensitive clays have occurred along the watercourses where erosion acted as the main triggering factor. Quinn et al. (2011, 2012) stated that the development of a failure surface in a sensitive clay landslide might be very slow (years of small erosions) or rapid (earthquake, pile driving, blasting, or other sudden shocks) depending on the triggering factor. However, if a slope has marginal stability, a small increase in stress in the slope (e.g., due to seasonal variation of pore water pressure) can cause a catastrophic failure (Lefebvre 1996; Quinn et al. 2011; Urmi et al. 2022). Various hydrological factors, including precipitation, piezometric pressure, groundwater flow, and other processes, are recognized as contributors to triggering retrogressive failures in sensitive clays (Donovan 1978; Eden and Mitchell 1970; Lefebvre 1986). Case studies and discussions of large landslide events in glaciomarine clay often identify hydrogeological factors, such as rainfall, snowmelt or anomalous weather leading up to the event, as a possible trigger (Evans and Brooks 1994; Karrow 1972).

Different authors tried to classify landslides in the presence of sensitive clays. Varnes (1978) identified two kinds of landslide, "spreading by lateral failure" and "earth flow" if the mass slides or flows, respectively. Carson and Lajoie (1981) classified the landslides in the sensitive marine sediments into five categories: two-dimensional spreading failures, aborted retrogression, excess retrogression, multidirectional retrogression, and flakeslides. The last four are comparable to the earth flows defined by Varnes (1978). Tavenas (1984) and Karlsrud et al. (1984) classified the landslides observed in the sensitive clays of Canada and Scandinavia based on the type of movement involved in the slides as single rotational slides, multiple retrogressive slides (earth flows/flow slides), translational progressive flake slides, and spreads. Locat et al. (2011) identified the last three types to occur suddenly and affect large areas. Hungr et al. (2014) updated Varnes's (1978) classification into 21 separate categories, among which landslides observed in sensitive clays are divided into sensitive clay flow-slides (multiple retrogressive slides/earth flows) and sensitive clay spreads (translational progressive flake slides). The following two subsections present a literature review on the two most important mechanisms: flow slides and spreads in sensitive clay.

Although spreads and flow slides are well distinguished in the literature, there is no clear agreement on how to differentiate their occurrence based on the material properties and characteristics of the slope. Demers

et al. (2014) analyzed the characteristics of historically recorded flow slides (over 60) and spreads (about 40) and showed similar material properties for both mechanisms. Some researchers pointed out that spreads can occur in soils with low sensitivity where a flow slide will not occur (Carson 1977; Demers et al. 2014; Locat et al. 2008). Quinn et al. (2007) suggested that spread occurs where the thickness of the crust is larger compared to the sensitive clay layer; thus, the remolded clay flows underneath and squeezes up through the cracks. In the event of flow slides, the upper crust is relatively thin compared to the sensitive clay layer; hence the crust is carried away with the remolded clay. Demers et al. (2014) found that spreads occur when the sensitive clay layers exist below the watercourse level, contrary to flow slides.

Flow slides

Flow slides initiate with a single rotational failure that is usually a result of a slow decrease of the shear strength in the sensitive clays due to leaching out of salt through pore water in the process of erosion over decades (i.e., drained conditions) (Bjrrum 1955). Consistently, the initial failure should be analyzed in drained conditions except for the cases when it is initiated by sudden loading (e.g. earthquake or intense rainfall). In soils that are not sensitive, the initially mobilized mass rapidly becomes stable (Fig. 5a, b). However, in sensitive clays, the shear strength within the failure surface and the deformed mass reduces dramatically down to the remolded shear strength (Fig. 5c). When the soil mass becomes remolded, it behaves like a viscous liquid (debris) and flows out of the newly formed crater with a considerable velocity. This movement and stress redistribution trigger a series of retrogressive rotational failures (Fig. 5d). The rapid removal of lateral support combined with the low permeability of the sensitive clay generates negative excess pore water pressures in the back scarp (i.e., undrained conditions) increasing the effective stress (Mitchell and Markell 1974). Therefore, each successive retrogression must overcome a greater average shearing resistance due to the changing initial stress conditions as the back scarp becomes further removed from the initial slope. Eventually, the back scarp remains stable, no more debris can flow out, and the sliding mass stabilizes (Fig. 5e).

Mitchell and Markell (1974) estimated that the transition between drained and undrained conditions happens at a horizontal distance from the toe of the slope between 3Hsecβ and 4Hsecβ (H being the slope height and β the slope angle) because the stresses within the slope drastically changes from K_0 condition at the mentioned horizontal distance. Therefore, the authors suggested that, for a failure starting in drained condition, retrogression beyond a horizontal distance of 3Hsecβ to 4Hsecβ from the toe of the slope should be considered as an undrained or short-term failure. For the undrained analysis, a flow slide occurs if the stability number, $N_s = \gamma H/s_{up}$ is larger than 6 (γ being the soil's natural unit weight and s_{up} the undrained shear strength), and it terminates due

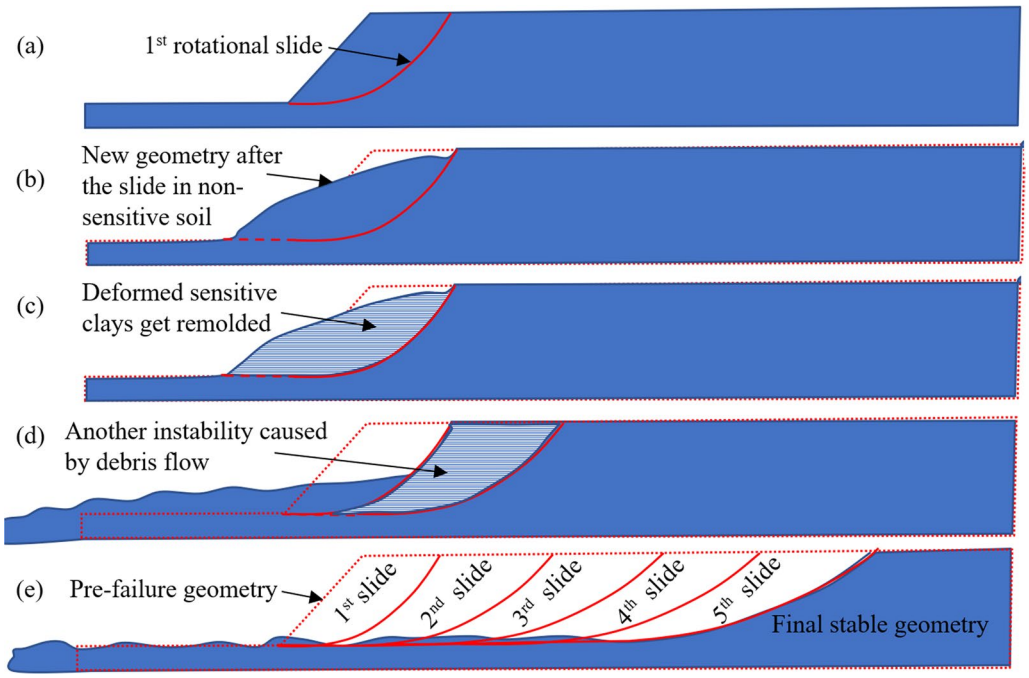

Fig. 5 **a**–**e** Flow slide mechanism (after the description of Bjrrum 1955)

to topographic/stratigraphic restrictions or when the energy dissipated in the flowing debris becomes equal to the energy released at the back scarp.

Other studies on flow slides in sensitive clays focus on the criteria for the occurrence of large retrogressive landslides. Lebuis and Rissman (1979) stated that large retrogressive landslides occur if the liquidity index (I_L) is greater than 1.2 or the remolded shear strength (s_{ur}) is less than 1 kPa. Tavenas et al. (1983) argued that the condition based on mechanical soil parameters is necessary for assessing retrogression potential but is inadequate. One must account for whether the energy dissipated by the initial slide is large enough to remold the clay so that it can flow out of the crater. They summarized all the conditions to assess retrogression potential in four points. Firstly, an initial slope failure must occur against long-term stability. Secondly, the back-scarp failure in undrained conditions will occur only if $N_s > 4$. Thirdly, the deformed soil mass from the first slide will get remolded if the remolding index (I_r) > 70% or liquid limit (w_L) < 40%. Finally, the remolded debris will flow if $I_L > 2$ or $s_{ur} < 1$ kPa. Lebuis et al. (1983) also stressed that the energy required for the clay to be wholly remolded should be dissipated from the first slide. They added another observation from case studies that earth flows with retrogression of 100 m occurs when the sensitivity (S_t) is greater than 25 and remolded shear strength (s_{ur}) is less than 1 kPa. Later studies somewhat agree with the previous criteria for large retrogressive failure.

For example, Lefebvre (1996) stated that slopes with Ns > 6 and $s_{ur} < 1.5$ kPa have the risk of retrogressive failure after an initial slide; Thakur and Degago (2012) stated that soils having $s_{ur} > 1$ kPa are less likely to initiate large retrogressive failure. Demers et al. (2014) showed by analyzing the previously occurred flow slides that most sites had very low remolded shear strength (< 0.8 kPa) and a very high liquidity index (1.5–16). To summarize, the aforementioned researchers acknowledged that large flow slides are most likely to occur when the following conditions are met: $S_t > 25$, $N_s > 4$, $w_L < 40\%$, $I_L > 1.2$, and $s_{ur} < 1$ kPa.

Spread

Spreads are identified by their unique structure of alternative crests and level surfaces after failure, generally known as horst and grabens (Fig. 6). The mechanism of spread was first described as a retrogressive failure by Odenstad (1951) for the Skottorp landslide in the Lidan river. Odenstad (1951) stated that the slide started with a part of the riverbank slipping into the river. The driving factor for the failure initiation was not distinctly identified, but erosion, leaching of salt, or blasting activity near the river could be responsible for the slow reduction of the slope stability over time. The formation process of horst and grabens is depicted in Fig. 6. When a slope experiences instability, the strength of the weak soil layer drops due to stress concentration within this layer and failure propagates horizontally through the layer opposite to the river producing a slide bottom "ba", simultaneously, a slip surface "bc" is formed at an angle of 45° parallel to the riverbank (Fig. 6a). When stresses along "bc" reach near to zero it starts to slip forming a wedge "bb'c'c" (Fig. 6b). When "bb'c'c" slips from position 1 to 2, it stops at a depth where it reaches the slide bottom forming a graben (Fig. 6c). The drag of this slip causes a rupture "de" parallel to "bc". By this time, the

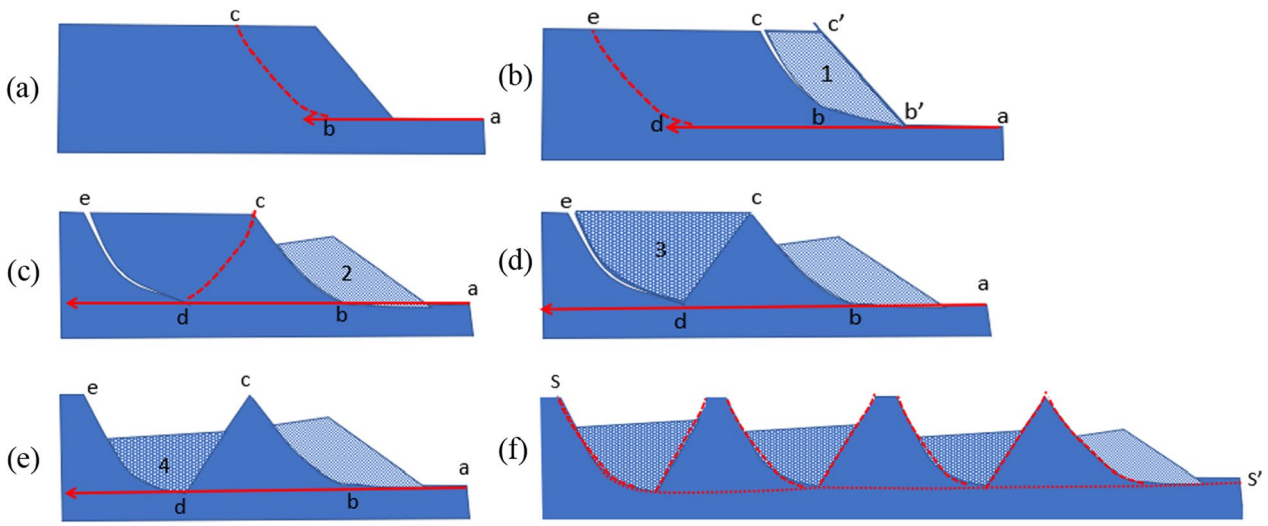

Fig. 6 **a**–**f** Spread mechanism (after Odenstad 1951)

slide bottom has already reached point "d" (Fig. 6c). The horizontal drag and vertical slip cause a secondary failure surface along "cd" creating a wedge "cde" (Fig. 6d). The wedge "cde" sinks from position 3 to 4, creating a graben which leaves a horst at "bcd" (Fig. 6e). This is how the whole strip "SS'" forms in a retrogressive and discontinuous manner (Fig. 6f) and finally slips into the river with an almost horizontal (slightly inclined towards the bottom) translatory movement.

Mollard and Hughes (1973) argued that the landslides in the Grondines and Trois Rivieres Areas, Quebec, explained by Karrow (1972) as multiple rotational retrogressive slides are instead a spreading failure. They reasoned that earthflow cannot explain the formation of parallel ridges. Their description agrees with Odenstad (1951) that the trigger for the initial instability could be any of the natural or anthropogenic reasons and that there exists a weak sensitive clay layer below the ground surface.

Unlike Odenstad's horizontal propagation of the slide bottom, they stated that with appreciable stress concentration, the sensitive clay layer gets remolded and spreads laterally like a liquid (Fig. 7a–c). The remolded clay is squeezed up through the cracks towards the top layer, and the top layer is stretched and separated into segmented blocks (Fig. 7b), which might have some rotational movements due to frictional drag. This produces ridge or rib-like patterns (Fig. 7c). The failure stops with the increased frictional resistance of the squeezed-up liquid and increasing strength due to pore pressure dissipation in the soil (Fig. 7d). Mollard and Hugh's explanation lacks the detailing of the influence of the tension cracks to create the prism-like structures in a spread.

Carson (1977) modified Odensta's (1951) spread mechanism and described the development of tension cracks in addition to horizontal subsidence (Fig. 8). He analytically explained the mechanism of the squeezed-up remolded clay in tension cracks aiding the formation of horst and grabens, combining both descriptions above. He postulated that the width of the cracks filled up with remolded clay at the end of the landslide equals the total volume of remolded clay in the weak layer. He emphasized that spread could occur regardless of the sensitivity

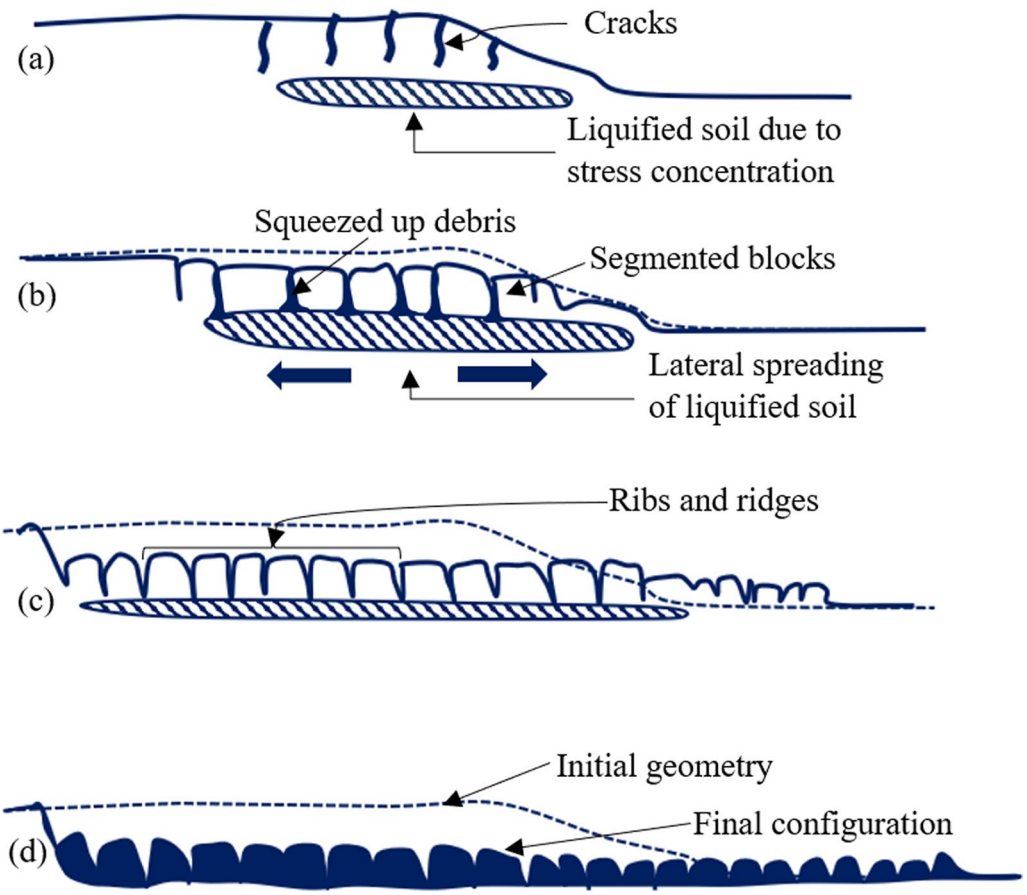

Fig. 7 **a**–**d** Mechanism of spread (after Mollard and Hughs 1973)

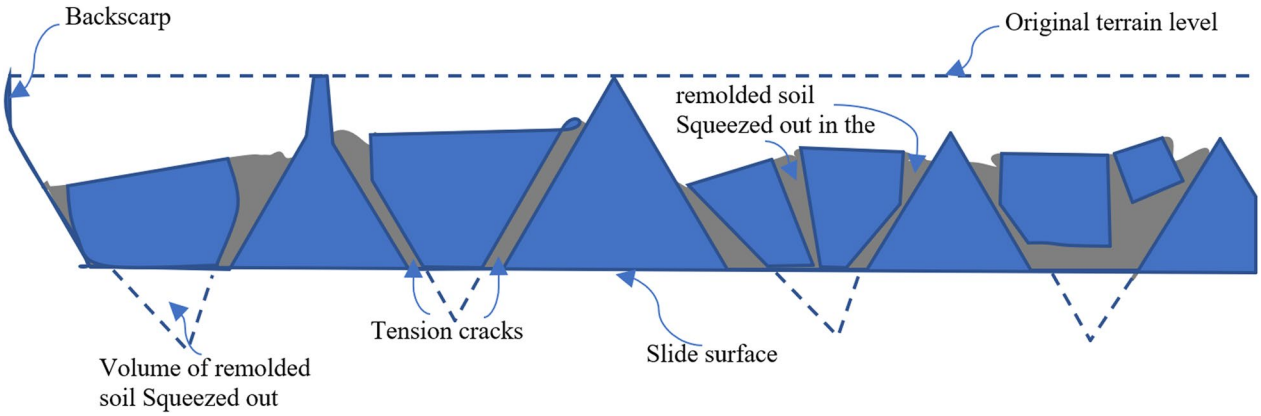

Fig. 8 Spread mechanism (after Carson 1977)

Fig. 9 Saint-Ligouri landslide (after Leroueil et al. 2011)

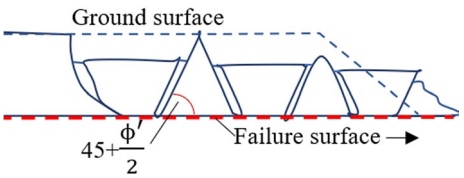

Fig. 10 Spread mechanism (after Locat et al. 2011)

being high or low; the important factor is how rapidly the soil gets disturbed to generate a rapid flow.

Grondin and Demers (1996) suggested that the formation of horst and grabens may not be discontinuous as the description by Odenstad (1951) and Carson (1977) because, in the landslide of St-Ligouri, the top surface of the grabens was connected by grass (Fig. 9). They suggested the landslide occurred due to horizontal subsidence that caused the dislocation of the upper soil mass.

A well-described discussion on the mechanism of spread can also be found in Locat et al. (2011). They described this mechanism as progressive (upward progressive failure) rather than retrogressive (Locat 2007; Quinn et al. 2007). As per their hypothesis, a failure surface in the sensitive clay layer, almost horizontal to the ground, moving upward starting near the toe of the slope, is formed before any noticeable movement occurs. The failure initiates with a slow translational movement of the soil mass above the failure surface. Then, the sensitive clay along the failure surface becomes remolded and liquefies due to the accumulated deformation. The movement accelerates the translational slide. Finally, the rapid progression of the soil mass above the liquified clay results in horst and grabens (Fig. 10).

Numerical analysis of sensitive clay landslides

Numerical modeling of sensitive clay landslides should address three particular challenges: strain-softening, remolding (solid to liquid transition), and large deformations. The following subsections present and discuss the prospect of the constitutive soil models and numerical frameworks considered in the literature to model sensitive clay landslides.

Constitutive soil models for the study of sensitive clays

The constitutive soil model, which represents the stress–strain behavior of the soil, is the most critical component for modeling sensitive clay slopes. The capability to reproduce realistic strain-softening characteristics in the material model is necessary for more accurate numerical analyses of large deformation problems in such materials. The constitutive models used in previous works for modeling sensitive clay landslides are summarized below. Their ability to deal with (a) strain-softening behavior, (b) strain-rate effects, and (c) rheological behavior of remolded soil is discussed. For completion, stress–strain curves numerically predicted by some of the models are compared with DSS data from sensitive clays. In particular, those constitutive models that have been used in the

literature to reproduce real case scenarios with available stress–strain DSS curves such data are considered for comparison (Locat et al. 2015; Tran and Sołowski 2019; Zhang et al. 2020). Otherwise, the stress–strain curve of Saint-Barnabé-Nord (Locat 2007) is considered for reference.

Von-Mises based models

The Von-Mises model is one of the simplest elastoplastic models to simulate the undrained behavior of clay. The model generally considers associated plastic flow and, at failure, it does not allow for volumetric strain. It requires only two parameters: the undrained elastic modulus (E_u) and the undrained shear strength (s_u). The Poisson's ratio is assumed constant ($\nu_u = 0.5$). Wang et al. (2016a, 2016b) used this model to simulate retrogressive failure features in sensitive clays together with a strain-softening law (Eq. 1), where the undrained shear strength linearly reduces with deviatoric plastic shear strain ($\bar{\varepsilon}_p$) from the peak (s_{up}) to a residual value (s_{ur}) (Fig. 11a).

$$s_u(\bar{\varepsilon}_p) = \begin{cases} s_{up} + H\bar{\varepsilon}_p; & \bar{\varepsilon}_p < \bar{\varepsilon}_{pr} \\ s_{ur}; & \bar{\varepsilon}_p > \bar{\varepsilon}_{pr} \end{cases} \quad (1)$$

where $\bar{\varepsilon}_{pr}$ is the plastic deviatoric strain at the onset of the remolded strength, and H is the linear softening coefficient.

The capacity of this model to reproduce the stress–strain curve of Saint-Barnabé-Nord (Locat 2007) is presented in Fig. 12b. For the determination of the softening modulus, the value of the strain at

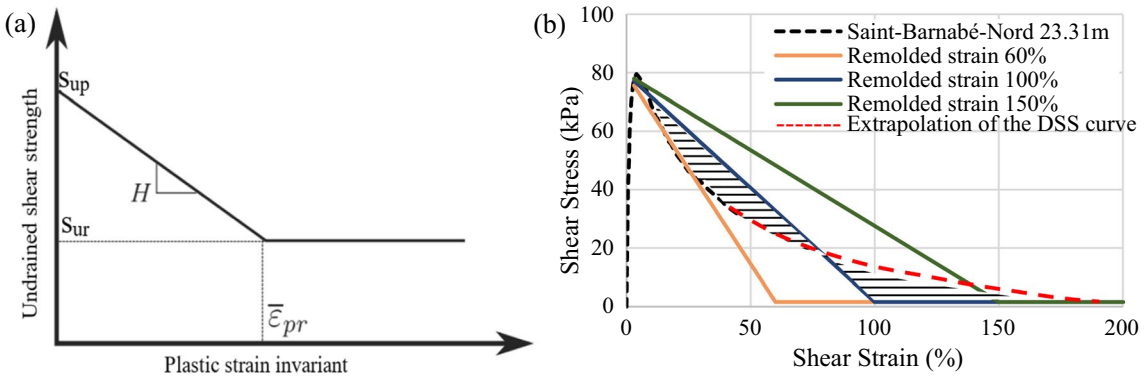

Fig. 11 **a** Stress–strain behavior in a cohesion softening model (Wang et al. 2016b, 2016a) **b** comparison between Wang et al.'s (2016b, 2016a) model and Saint-Barnabé-Nord clay

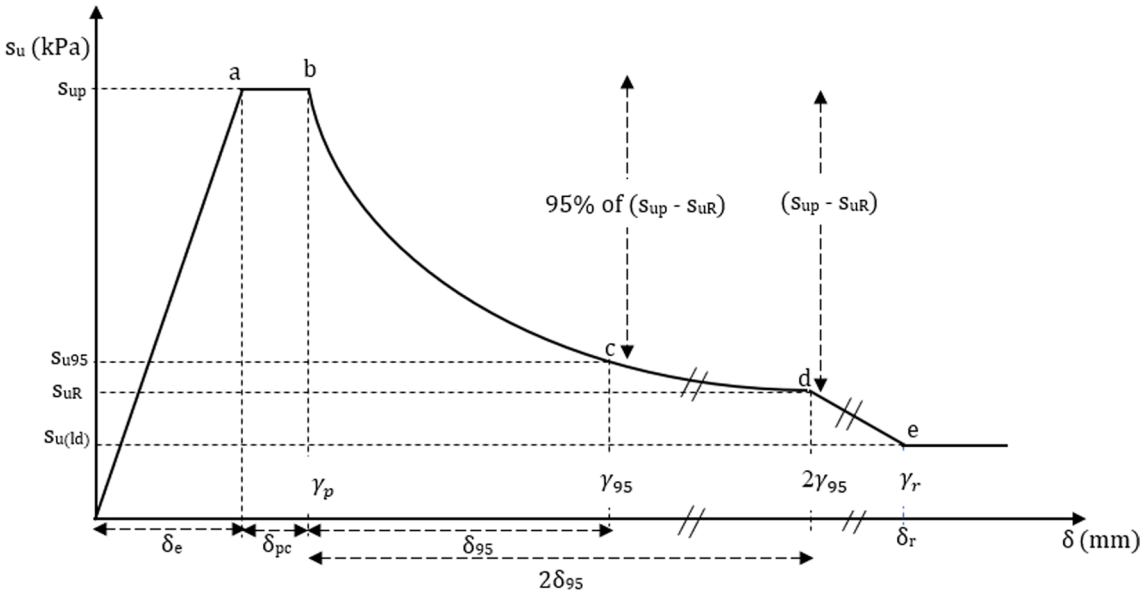

Fig. 12 Stress–strain behavior of sensitive clay (Dey et al. 2015)

remolded shear strength is required. Based on Thakur and Degago (2014), the strain at remolded shear strength is estimated to be 300% for Norwegian sensitive clays. Assuming the strain at remolded shear strength as 60–150% and considering $s_{up} = 79.5$kPaand $s_{ur} = 1.6$kPa based on the experimental results from Locat et al. (2008), the value H varies between −135 to −52 kPa. It is observed from Fig. 11b that the linear approximation either overpredicts or underpredicts the actual curve obtained from laboratory testing. Even though a linear approximation cannot capture the nonlinearities of the softening behavior of sensitive clays, a reasonable approximation can be achieved when the areas between the stress–strain curves produced by the constitutive model and the actual stress–strain curve compensate (e.g., the case with remolded strain taken as 100%).

A group of researchers (Dey et al. 2016a, 2016b, 2015; Islam et al. 2019) used the same yield criterion with a non-linear strength degradation as a function of plastic shear displacement (Fig. 12) as follows,

$$\frac{s_u}{s_{up}} = \begin{cases} \frac{s_{uR}}{s_{up}} + \left(1 - \frac{s_{uR}}{s_{up}}\right) e^{-\frac{3\delta'}{\delta_{95}}} & if \;\; 0 \le \delta' < 2\delta_{95} \\ \frac{s_{uR}}{s_{up}} - \frac{s_{uR} - s_{ur}}{s_{up}} \frac{\delta' - 2\delta_{95}}{\delta_r - 2\delta_{95}} & if \;\; 2\delta_{95} \le \delta' < \delta_r \\ \frac{s_{ur}}{s_{up}} & if \;\; \delta' \ge \delta_r \end{cases} \tag{2}$$

where s_u is the mobilized undrained shear strength; $\delta' = \delta_t - \left(\delta_e + \delta_{pc}\right)$ with δ_e and δ_t being the elastic and total shear displacements, respectively; δ_{95} is the value of δ' at which the undrained shear strength is reduced by 95% of $(s_{up} - s_{uR})$. s_{uR} is the degraded strength at a displacement of $2\delta_{95}$ after the peak.δ_r is the value of δ' remolded shear strength (s_{ur}).

The non-linear part of Eq. (2) (curve "bcd" in Fig. 12) is a modified form of the strength degradation equation proposed by Einav and Randolph (2005) as follows,

$$\frac{s_u}{s_{up}} = \frac{s_{ur}}{s_{up}} + \left(1 - \frac{s_{ur}}{s_{up}}\right) \times e^{-\frac{3\gamma}{\gamma_{95}}} \tag{3}$$

where displacements relate to the strain as $\delta = \gamma t$ (t = shear band thickness).

The linear-elastic pre-peak segment (line "oa" in Fig. 12) is defined using undrained stiffness parameters. The peak undrained shear strength (s_{up}) is mobilized at point "a" and remains constant up to point "b" for a displacement of δ_{pc} from point "a". The rest of the curve corresponds to Eq. (2).

The comparison between the post-peak stress–strain relationship predicted by Eq. (3) and the DSS stress–strain curve of Saint-Barnabé-Nord (Locat 2007) is presented in Fig. 13. The comparison has been made in terms of shear strain instead of displacement. After a calibration process, the most fitting curve is obtained with γ_{95}=130%. The predicted curve shows some discrepancies with the DSS data up to 20% strain, but it exactly matches from 20–46% strain.

It can be concluded that exponential strain softening is better suited than linear strain-softening laws to capture the strain-softening from sensitive clays, but much uncertainty prevails in the accurate estimation of the parameters like γ_r and γ_{95}. The wrong approximation of these parameters can significantly reduce the accuracy of the strain-softening equation for field conditions.

Wang et al. (2021, 2022) added strain-rate effects on the shear strength using Eq. (4). They considered the undrained shear strength (s_u) as a function of a shear strain-softening factor (f_1) and a strain rate factor (f_2) as

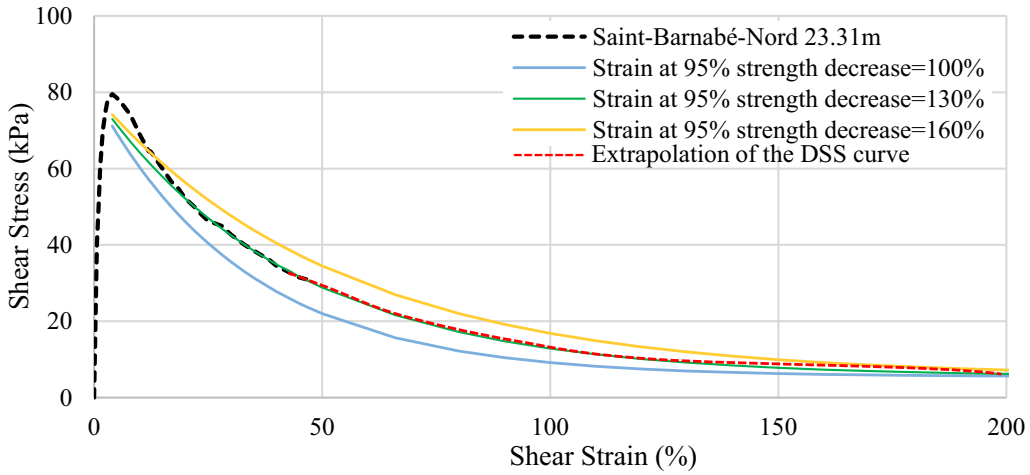

Fig. 13 Comparison between the exponential strain-softening law with different γ_{95} to the stress–strain behavior from DSS test from Saint-Barnabé-Nord clay

$$s_u = s_{uy}(f_1 f_2) \tag{4}$$

where s_{uy} is the undrained shear strength at a very low strain rate (i.e., quasi-static).

Generally, the dependency of undrained shear strength of clays on applied strain rate has customarily been characterized in terms of a semi-logarithmic relation (Graham et al. 1983; Zhou and Randolph 2009) (Eq. 5) and a power law (Eq. 6) (Einav and Randolph 2005) expressed as,

$$s_u = \left[1 + \mu log\left(\frac{\dot{\gamma}}{\dot{\gamma}_{ref}}\right)\right] s_{u,ref} \tag{5}$$

$$s_u = \left(\frac{\dot{\gamma}}{\dot{\gamma}_{ref}}\right)^{\beta} s_{u,ref} \tag{6}$$

where $\dot{\gamma}$ is the shear strain rate, $\dot{\gamma}_{ref}$ is the strain rate at a reference shear strength $s_{u,ref}$, the coefficient μ and β give the proportional change in shear strength for each order of magnitude change in strain rate, which lies in the range of 0.05–0.2 and 0.05–0.1, respectively.

Again, the behavior of liquified remolded sensitive clays in debris flow can be described with a strain rate dependent fluid mechanics framework (Herschel–Bulkley model) relating the yield stress (τ) with strain rate ($\dot{\gamma}$) based on fluid viscosity (η) and a shear thinning index (n) as (Deglo De Besses et al. 2003),

$$\begin{cases} \dot{\gamma} = 0 & for\ |\tau| \le \tau_0 \\ \tau = \tau_0 + \eta|\dot{\gamma}|^n & for\ |\tau| > \tau_0 \end{cases} \tag{7}$$

For the sensitive clays, the effect of strain rate on the undrained shear strength would be present in the solid phase as well as in the liquid phase when it flows like debris. To capture the strain rate effect on strength in both the phases Zhu and Randolph (2011) proposed a unified equation that originates from the power-law (Eq. 6) but also incorporates the viscosity and shear thinning index like Herschel–Bulkley model. This unified equation is termed an "additive power law" model and expressed as,

$$s_u = \left[1 + \eta\left(\frac{\dot{\gamma}}{\dot{\gamma}_{ref}}\right)^n\right] s_{u,ref} \tag{8}$$

Wang et al. (2021, 2022) used Eq. (8) in his constitutive model to incorporate strain rate, and the second function in Eq. (4) is defined as,

$$f_2 = \left[1 + \eta\left(\frac{\dot{\gamma}}{\dot{\gamma}_{ref}}\right)^n\right] \tag{9}$$

By incorporating strain rates, constitutive models can effectively evaluate the impact of a time-dependent strain or creep behavior on both the onset and advancement of failure.

Tresca based models

Tresca is also an elastoplastic model, very similar to the Von-Mises model. Its simplicity inspired some researchers to model sensitive clays by adding strain-softening laws (Shan et al. 2021; Tran and Sołowski 2019; Yuan et al. 2020; Zhang et al. 2015). Locat et al. (2013) modeled the spread mechanism in sensitive clays assuming a hyperbolic elasticity model up to the peak stress and linear plasticity in post-peak strain softening (Fig. 14a). The strain-softening is linear and defined with a softening modulus K_s as follows,

$$K_s = \frac{s_{up} - s_{ur}}{\delta_r - \delta_p} \tag{10}$$

where δ_p and δ_r are the shear displacement at peak and remolded strength, respectively.

This model has also been applied to study the post-peak behavior of the Sainte-Monique landslide in

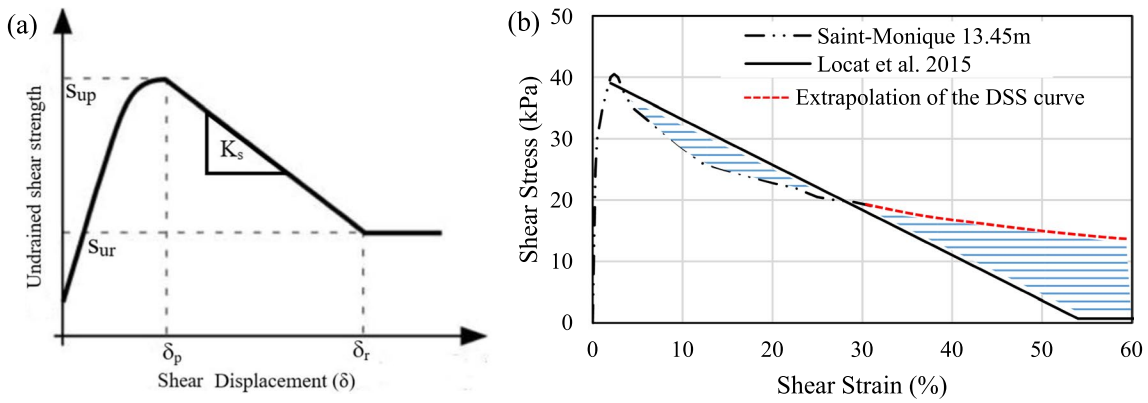

Fig. 14 **a** Shear stress-displacement relationship (Locat et al. 2013), **b** comparison of assumed strain-softening with the laboratory test result

Quebec (Locat et al. 2015), assuming $\gamma_p = 2\%$ and $\gamma_r = 55\%$. The comparison between the linear approximation and the measured stress–strain curve is presented in Fig. 14b. It is evident that linear approximations significantly deviate from the actual stress–strain curves.

Zhang et al. (2015) investigated the initiation and propagation of a fully softened shear zone in submarine sensitive clay landslides with both linear (Eq. 11) and non-linear (Eq. 12) strain-softening laws. The latest (Eq. 12) is based on Einav and Randolph (2005) (Fig. 15).

They compared the critical length of the softened zone predicted by the numerical model with the analytical evaluation and concluded that linear degradation overestimates the length of the shear band by 10–15% more than non-linear degradation. The softening equations are as follows,

$$s_u = s_{up} - \left(s_{up} - s_{ur}\right)\frac{\gamma}{\gamma_r} \tag{11}$$

$$s_u = s_{ur} + \left(s_{up} - s_{ur}\right)e^{-\frac{\gamma}{\gamma_{95}}} \tag{12}$$

where s_u is the degraded undrained shear strength at displacement increment γ after reaching the peak, and γ_{95} is the plastic strain increment required to reduce the strength by 95% of ($s_{up} - s_{ur}$) from the peak strength (s_{up}),

Shan et al. (2021) added strain-rate effects and depth-wise variation on shear strength to Eq. (11) as

$$s_u = max\left(s_{up} - \left(s_{up} - s_{ur}\right)\frac{\gamma}{\gamma_r}, s_{ur}\right)\left(1 + \overline{K}\left|\frac{\dot{\gamma}}{\dot{\gamma}_{ref}}\right|^n\right) \tag{13}$$

where n is the power index (usually varies from 0.4 to 0.6 for Canadian sensitive clay), and $\overline{K}$ is the viscosity coefficient ($\overline{K} \approx 0.028 s_{up}^{0.28}$). The depth-wise variation of peak strength was defined as follows:

$$s_{up} = \begin{cases} s_{up1} & 2m \le h < 5m \\ s_{up1} + a(h-5) & h \ge 5m \end{cases} \tag{14}$$

where h is the soil depth, s_{up1} is the undrained shear strength in the first clay layer (h =2 m-5 m), and "a" is the strength gradient along the depth h in the second clay layer (h >5 m).

Tran and Sołowski (2019) proposed a modified version of the elastoplastic Tresca model with a non-associated flow rule for modeling the progressive failure behavior of sensitive clays and used it to simulate the Sainte-Monique landslide. They added features to the model for replicating the field soil behavior, including strain-rate effects, the effect of water content, and soil depth on the shear strength. The non-linear strain-softening law describes the strength degradation as follows,

$$s_u = s_{u,ref}\left(\frac{\dot{\gamma}}{\dot{\gamma}_{ref}}\right)^{\beta}\left[\frac{1}{S_t} + \left(1 - \frac{1}{S_t}\right)e^{-3\gamma/\gamma_{95}}\right] \; when \; \gamma > \gamma_e \tag{15}$$

where γ_e is the accumulated elastic strain. The reference undrained shear strength depends on the water content (w) and depth (h) as:

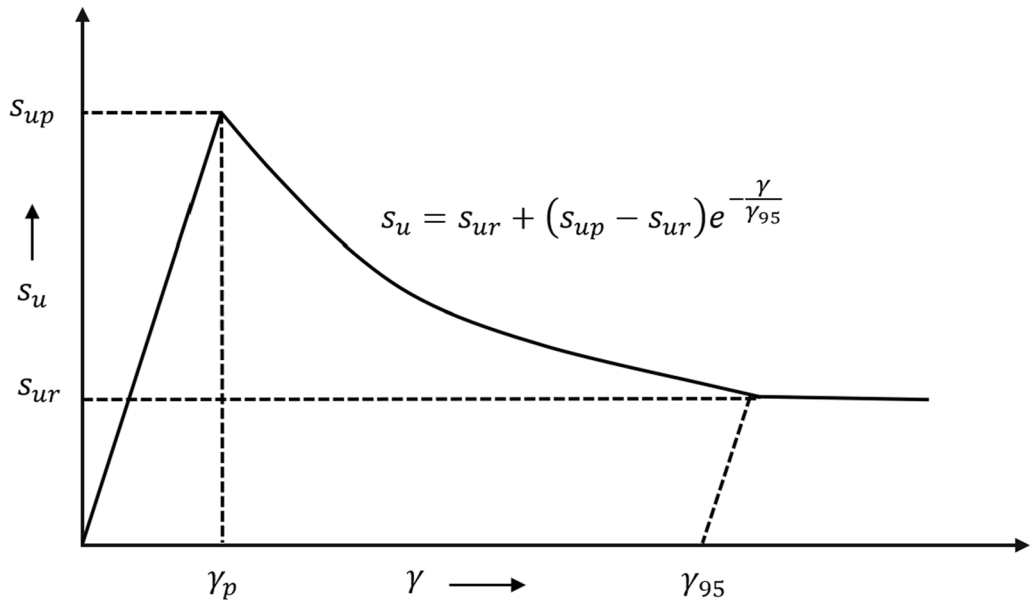

Fig. 15 Stress–strain behavior with exponential strain-softening (Zhang et al. 2015)

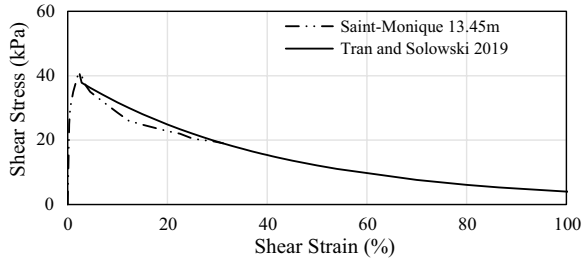

Fig. 16 Comparison of stress–strain behavior of DSS test result with the numerical model of Tran and Solowski (2019)

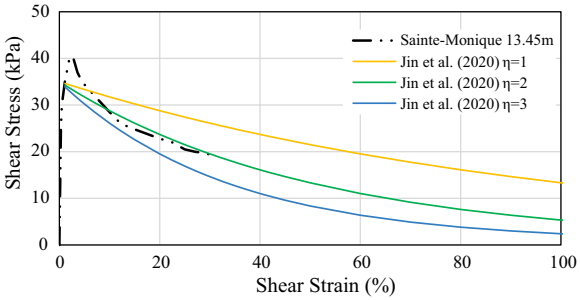

Fig. 17 Comparison between DSS test results vs. stress–strain behavior of Jin et al. (2020) with different η values

$$s_{u,ref}(w,h) = \left(a_1 w^{-b_1}\right)\left[s_{uh,ref} + \Delta s_u\left(h - h_{ref}\right)\right] \tag{16}$$

where, a_1 is the undrained shear strength at w = 100% at a reference strain rate (γ_{ref}), w (%) is the water content and b_1 is the model parameter, $s_{uh,ref}$ is the reference undrained shear strength at the reference depth h_{ref}, and Δs_u is the increase of strength per unit depth after the reference depth. The stress–strain prediction of this model is compared with laboratory DSS test result (Sainte-Monique landslide), which shows that this model is better suited compared to previous linear models discussed above in terms of capturing the non-linear stress–strain behavior of sensitive clays (Fig. 16).

Jin et al. (2020) simulated retrogressive failure in sensitive clays with a cohesion softening model which is comparable to the Tresca softening model where the peak and residual cohesion (c_p and c_r) are equivalent to the peak and remolded undrained shear strengths (s_{up} and s_{ur}) of sensitive clays. The softening is defined as,

$$s_u = s_{ur} + \left(s_{up} - s_{ur}\right)e^{-\eta\bar{\varepsilon}_p} \tag{17}$$

where η is the shape factor that controls the rate of strength decrease.

They evaluated mesh dependency and the effect of the shape factor η on post-failure behavior of the landslides. It can be seen in Fig. 17 that, the softening curve is significantly dependent on the value of the shape factor (η). For the case of Sainte-Monique landslide, $\eta = 2$ is more representative of the field behavior.

Bingham-Tresca based models

The constitutive models described above are common in the study of soil mechanics, and most of them do not directly consider the rheological properties of the clay, which may affect the prediction of runout distances in retrogressive flow slides. In the field of fluid mechanics, the Bingham plastic model is a common constitutive law that considers non-Newtonian rheology to predict the flow behavior using its yield stress (τ_y) and plastic viscosity (η). As shown in Fig. 18, the fluid starts to flow after reaching its yield stress, and the yield stress increases linearly with the shear rate. Several rheological models have been used for simulating the debris flow of sensitive clays, including the Herschel–Bulkley model (Imran et al. 2001; Turmel et al. 2020; Turmel and Locat 2018). The Bingham model is a limiting case of Herchel–Bulkley rheology. It should be noted that these models only consider the liquid flow of the sensitive clays and do not capture the transition from solid to a liquid phase.

With the idea of capturing the transition from solid to liquid behavior of sensitive clay, Zhang et al. (2017) came up with an elastoviscoplastic model that combines an elastoplastic model with a viscous model using the concept of strain-based transition initially proposed by Prime et al. (2014). In particular, they combined the Bingham model and the Tresca model with linear strain softening (Zhang et al. 2018, 2020, 2017). Total strain rate ($\dot{\varepsilon}$) for the elastoviscoplastic material is defined as the summation of an elastic strain rate ($\dot{\varepsilon}^e$) and a viscoplastic strain rate ($\dot{\varepsilon}^{vp}$).

$$\dot{\varepsilon} = \dot{\varepsilon}^e + \dot{\varepsilon}^{vp} \tag{18}$$

The strain is purely elastic when the stress state is below the Tresca yield surface, whereas viscoplastic strain starts to develop when the stress state crosses the yield surface. Strain softening is incorporated by reducing

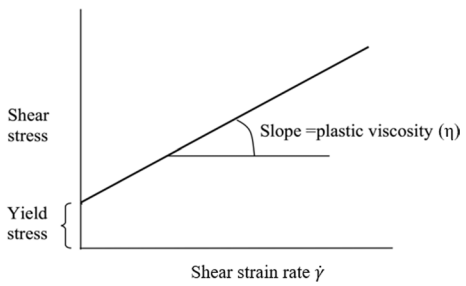

Fig. 18 Bingham plastic model

the undrained shear strength s_u using a bilinear function (similar to Fig. 11a) of the equivalent deviatoric plastic strain. In this case, the softening modulus H is a function of the viscoplastic strain (ε^{vp}).

The classical Bingham model is utilized to describe the rheological behavior of sensitive clays, and the total stress is defined as,

$$\sigma = \tau + \eta \dot{\varepsilon}^{vp} \tag{19}$$

where τ is the stress lying on the boundary of the Tresca yield surface, η is the viscosity coefficient and $\dot{\varepsilon}^{vp}$ is the viscoplastic strain. When the viscosity is zero, the model reduces to the classic Tresca model. This model is comparable to the strain-rate-based models, where the strain-rate dependency of liquified debris is derived from the Herschel–Bulkley model (Eqs. 7–9). Zhang et al. (2019) used this constitutive soil model to simulate the Saint-Jude landslide (2010) and showed that ignoring rheological properties overestimates the runout distance. However, the linear strain-softening is not representative of the actual stress–strain behavior (Fig. 19).

Numerical frameworks for modeling landslides in sensitive clays

Numerical analysis has two prominent approaches, i.e. continuum mechanics and discrete mechanics. In continuum analysis, each particle within a material is not treated explicitly, and the material is modeled as a continuous entity; the change in the properties of the geomaterial under loading conditions is represented by a constitutive model. On the other hand, discontinuum methods model the geomaterial as a collection of distinct particles which may or may not represent a real particle arrangement, and the particles interact through their contacts with other particles and boundaries. Numerical analysis for large deformation problems in geomechanics has been a prominent issue in recent times. Both continuum and discontinuum numerical frameworks for modeling geomaterials, particularly for large deformation problems, have been summarized by Augarde et al. (2021). Before that, Soga et al. (2016) and Wang et al. (2015) compared the advantages and disadvantages of existing numerical frameworks used in slope stability analysis and other geotechnical problems, respectively. In the following section, large deformation numerical frameworks that have particularly been used in the analysis of landslides with strain-softening materials or sensitive clays will be discussed, which are mainly different formulations in continuum approaches.

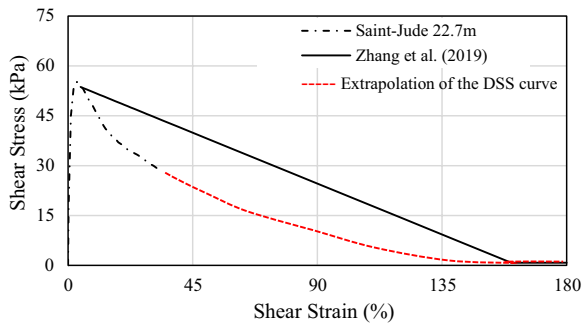

Fig. 19 Comparison between DSS test results vs. stress–strain behavior of Zhang et al. (2017)

Updated Lagrangian finite element method

The most popular approach used in geotechnics is the standard finite element method (FEM) with classic Lagrangian formulation (known as the total Lagrangian, TL). The TL is a continuum method that uses the undeformed initial geometry as its frame of reference for computing the static and kinematic variables as well as formulating the discrete equations. In the cases where deformations are substantial with respect to the initial geometry, this formulation suffers from mesh distortion and produces inaccurate results. The updated Lagrangian (UL) formulation is an upgraded version of the classic lagrangian formulation to solve the mesh distortion problem for its implementation in large deformation problems (Bathe 1996). In UL formulation, the variables are computed, and equations are formulated for the deformed state in the previous calculation step. Therefore, the positions of the nodes are updated based on the displacement calculated in the last increment. The UL framework is available in some commercial FEM software, making it flexible to work with. The limitation of this method is that when very large deformation is encountered, elements become too distorted. This distortion reduces the accuracy of the results and creates computational instabilities that make the calculation impossible (Augarde et al. 2021). Mohammadi and Taiebat (2013) have used the UL FEM formulation to simulate progressive failure in strain-softening soil slopes. In their model, mesh distortion was encountered for higher sensitivity ($RF = 1/S_t$), as shown in Fig. 20.

Arbitrary Lagrangian–Eulerian (ALE) methods

ALE is the upgraded version of UL, which offers a solution to the mesh distortion by substituting the distorted mesh with a new mesh (re-meshing). This requires the transfer of state variables (re-mapping), which might reduce the accuracy of the solution when these are history-dependent. This method is referred to as arbitrary Lagrangian–Eulerian because the process of material state transformation from the old mesh to the new one is similar to that of the Eulerian description. Several

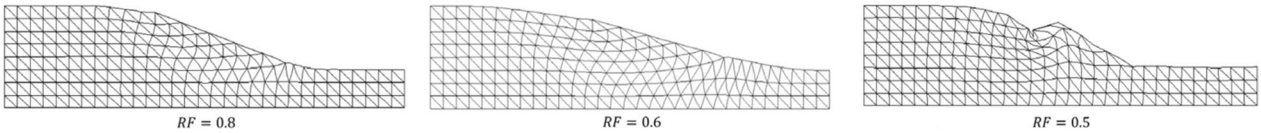

Fig. 20 The deformed FEM mesh for different RF values with UL (after Mohammadi and Taiebat 2013)

re-meshing and re-mapping methods have produced several branches of the ALE formulation. The Re-meshing and Interpolation Technique combined with Small Strain (RITSS) approach is a widely popular re-meshing technique. The RITSS approach addresses large strain problems by dividing them into smaller Lagrangian strain increments (Hu and Randolph 1996). At the end of each increment, the deformed body is re-meshed with new undistorted elements. To ensure an accurate transfer of information, solution variables such as stresses, deformations, velocities, nodal pore pressures, etc., are then interpolated from the old mesh to the new mesh (Ullah et al. 2018). The RITSS process can be broken down into four main steps, which include the generation of an initial mesh, conducting an incremental step of the Lagrangian analysis, updating boundaries and re-meshing, and mapping stresses and material properties from the old to the new mesh. These steps are repeated until the entire large deformation analysis is completed using a standard Lagrangian finite element package (Tian et al. 2014). This process, thus, overcomes mesh distortion and allows for the modeling of various geotechnical problems, including those with fully drained, undrained, or intermediate drainage conditions. It's important to note that the accuracy and success of this process depend on the choice of interpolation scheme and mesh density. The RITSS approach can be flexibly used in any FEM code but is computationally very expensive. Zhang et al. (2015) used the RITSS approach to simulate the initiation and propagation of a shear band in a fully softened weak zone. Zhang et al. (2019) simulated a landslide in submarine sensitive clays with the same framework. Shan et al. (2021) simulated the Sainte-Monique landslide in Quebec in 1994 with RITSS and successfully simulated some features of the retrogressive failure.

One of the most popular versions of ALE is the Coupled Eulerian–Lagrangian (CEL) method, also known as multi-material ALE. This method utilizes the advantages of both the Lagrangian and Eulerian approaches (Qiu et al. 2011). This method has two different domains for material description. One is the classic Eulerian, and the other is the updated Lagrangian. Stiffer materials are described with the Lagrangian domain. When stresses are applied on these stiffer materials, it causes the softer materials in the vicinity to experience large deformation. The Eulerian description allows these softer materials to deform freely. The two domains interact with each other through some contact algorithms. The CEL approach is also available in commercial software like ABACUS. Dey et al. (2013, 2015, 2016a, 2016b) used this framework to model progressive failures leading to spreads in submarine sensitive clay slopes. Islam et al. (2019) used this framework to model retrogressive failure initiated by earthquake loads. Wang et al. (2021, 2022) modeled retrogressive failures resulting from erosion with some practical applications using this method. The authors adapted the techniques to reduce the mesh dependency of the models.

Particle finite element method (PFEM) and smoothed particle finite element method (SPFEM)

The Particle Finite Element Method (PFEM) is also an approach mainly developed to overcome the mesh distortion suffered by FEM. In this method, the mesh nodes are regarded as particles that can freely move even beyond the initial computational domain. The particles carry all information. The boundary of the domain is marked by connecting the outermost particles, and each internal particle is connected through the Delaunay triangulation technique. After the mesh is established, the governing equations are solved as it is in a conventional FEM simulation. The updated positions of the mesh nodes are used to form a new cloud of particles, and the process repeats (Fig. 21).

The main advantage of this method is that it shows convergence behavior regardless of a large change in the state variables from the previous calculation step to the current step, which is very useful for modeling history-dependent materials like sensitive clay landslides (Zhang et al. 2018, 2017). Zhang et al. (2020) utilized this framework to simulate the Saint-Jude landslide in Quebec, Canada. It has been able to reproduce the failure mode and the progressive failure process of the Saint-Jude landslide and correctly estimated its final runout distance, retrogression distance, and failure surface. The infinitesimal strain assumption in this method is likely to result in several errors, including excess strain for rigid body motion. Zhang et al. (2017) reported that the error is limited to 1% for a converged solution. Contact between solid–solid and solid–liquid is complex in this method. Frequent re-meshing in large deformation problems requires extreme precision in transferring history-dependent information

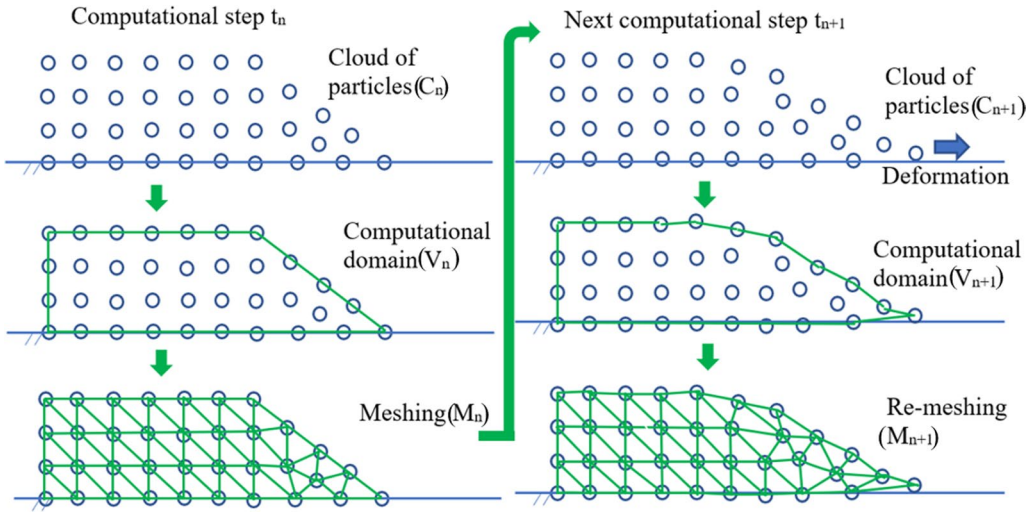

Fig. 21 Steps for the PFEM modeling of a landslide

from the old mesh to the new one to maintain the accuracy of the calculation (Augarde et al. 2021).

The Smoothed Particle Finite Element Method (SPFEM) is an improved form of PFEM where the equilibrium of the governing equations is established at the nodes instead of the Gaussian points with the help of strain smoothing cells covering each node. This reduces the error in re-mapping the history-dependent variables. This method is more accurate and computationally flexible than PFEM (Zhang et al. 2018). With this framework, Yuan et al. (2020) simulated retrogressive failure in sensitive clays. This simulation used the simplest form of the strain-softening Tresca model. Therefore, the applicability of this framework with a more sophisticated constitutive model with rate effects and non-linear softening is yet to be studied.

Material point method (MPM)

MPM is a combination of particle-based and mesh-based methods. The computational domain is discretized with a number of particles (i.e. material points) and a fixed background mesh. The material points are described in the Lagrangian formulation. Each material point represents a part of the computational domain and moves through the fixed background mesh. All the physical properties of the continuum are carried by the material points. The background mesh is described in Eulerian formulation. The state variables are transferred from the material points to the mesh nodes in each computational step (Fig. 21: Steps for the PFEM modeling of a landslide Fig. 22), and the balance equations are solved at the nodes of the Eulerian mesh. Updated properties are mapped back to the material points, and the calculation proceeds to the next step. The background mesh must contain the problem domain geometry, and the material deformation is carried by the material points. Thus, the mesh remains undistorted throughout the calculation, and mesh distortion is completely avoided. Some numerical difficulties of MPM are cell crossing instability, generation of non-physical stiffness, and the mapping from material points to nodes and back.

The full process of retrogressive failure of sensitive clay triggered by erosion has been simulated using MPM framework by Wang et al. (2016b, 2016a) and Tran and Sołowski (2019). The simulations well captured the features of a retrogressive landslide.

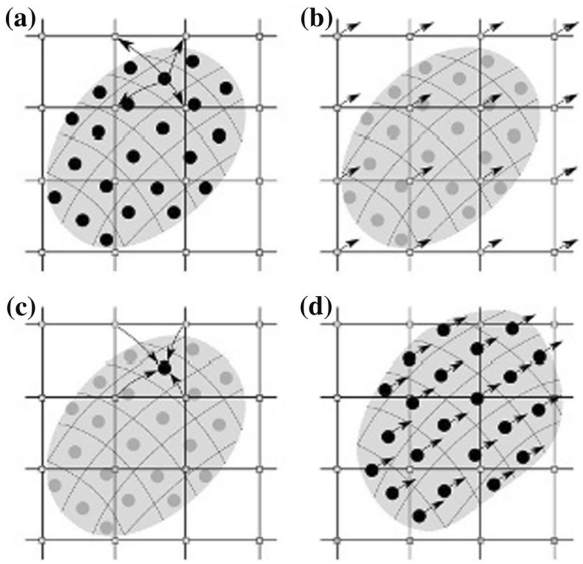

Fig. 22 MPM Computational cycle (Fern et al. 2019)

Contribution of numerical analysis to understand the control parameters of sensitive clay landslides

Various combinations of the constitutive models and numerical frameworks described in the previous section have been implemented to model different landslides in sensitive clays. Some of these works explore the failure mechanisms in detail and provide new insights. Numerical simulations also help understand which geometrical and material parameters control the occurrence and post-failure behavior of sensitive clay landslides. The following section focuses on how the numerical results aided in understanding the critical factors for sensitive clay landslides.

Effect of the geometry of the slope on the occurrence and post-failure behavior

Several numerical studies have evaluated how the geometrical variations of the soil layer or the slope change the failure pattern, retrogression, and runout distances. In particular, the effect of the thickness of the sensitive clay layer, height and width of the slope, slope angle, and inclination of the soil layer are some aspects that have been assessed.

Dey et al. (2016b) showed that a minimum thickness of the sensitive clay layer is required to initiate retrogressive/progressive failure, while Zhang et al. (2020) concluded that an increase in the thickness of the sensitive clay layer (H_{St}), keeping the crust thickness constant, increases retrogression distance. Additionally, an increase in H_{St} changes the failure pattern from spread to flow slide (Dey et al. 2015; Islam et al. 2019). Studies show that for a fixed slope height, an increase in slope width increases the retrogression and runout up to an optimum value. After this point, further width increase results in no significant change in post-failure behavior; that is, slope width has an optimum value for the occurrence of large retrogressive failure (Yuan et al. 2020). The frictional coefficient of the base layer also controls the retrogression. It is observed that the larger the basal friction, the less susceptible the slope is to retrogressive failure (Wang et al. 2016a, b; Yuan et al. 2020). The slope angle controls the failure mechanism and post-failure behavior to a great extent. For a varying slope angle (β) of a horizontal soil layer (Fig. 23a), steeper slopes are more susceptible to larger retrogressive failure (Dey et al. 2016a, 2016b; Islam et al. 2019; Locat et al. 2013). Jin et al. 2021 showed that higher β value reduces the time to reach failure for sensitive clay slopes. For a varying inclination of the clay layer α with the horizontal (Fig. 23b), a higher α changes the slide movement from rotational to translational and produces a higher number of secondary slip planes with smaller failure blocks (Wang et al. 2016a, b). Islam et al. (2019) further demonstrated with a varying upslope inclination (γ) (Fig. 23c) that flow slide occurs for low and high values of γ. In contrast, the failure pattern for intermediate γ is spread. Overall, these numerical results align with the literature that the susceptibility and extent of progressive failure are high on steep slopes (Lo and Lee 1973).

Effect of material properties on the occurrence and post-failure behavior

The effect of different material parameters on the initiation and the extent (retrogression and runout distance) of the sensitive clay landslides has been assessed in light of different numerical simulations. Dey et al. (2015) showed that progressive failure would not occur for very low sensitivity ($S_t < 3$), spread occurs with medium sensitivity ($S_t \sim 5–7$), and the failure pattern changes to a flow slide with higher sensitivity ($S_t \geq 10$). Moreover, they found that decrease in the shear strength of the crust changes the failure pattern from spread to flow slides. In contrast, Islam et al. (2019) illustrated that the failure pattern changes from a flow slide to a combined spread and flow slide type with increased sensitivity. Even though both Dey et al. (2015) and Islam et al. (2019) used the same softening constitutive model and numerical framework, the differences in their conclusions might be due to the different triggering factors considered in their analysis, i.e., toe erosion (Dey et al. 2015) and earthquake (Islam et al. 2019). In any case, both works coincide in that higher sensitivity caused higher retrogression and runout distances. Zhang et al. (2018) illustrated that in addition to the increased

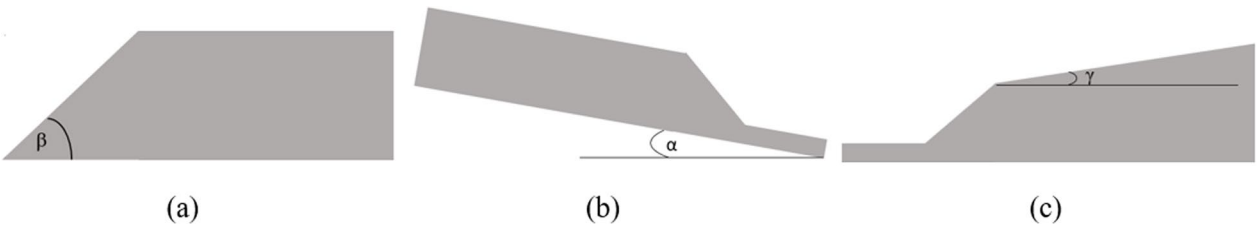

Fig. 23 Different types of slope inclination

retrogression and runout, it takes a longer time for the sliding front to stop entirely with increased sensitivity. Yuan et al. (2020) added that the failed soil mass would reach a longer runout distance with higher sensitivity, owing to a smaller dissipation of potential energy for remolding, leading to higher kinetic energy.

Tran and Sołowski (2019) showed that large retrogressive landslides are also dependent on low remolded strength (s_{ur}< 2 kPa) with high sensitivity (S_t > 25). Several researchers demonstrated that the retrogression distance is significantly controlled by the remolded shear strength. Increased remolded strength s_{ur} (keeping all other material and geometrical parameters fixed) reduces the retrogression distance, and a further increase in s_{ur} completely stops the retrogression (Islam et al. 2019; Locat et al. 2013; Tran and Sołowski 2019; Wang et al. 2016a, b). Likewise, when the remolded strength approaches zero, there is a sharp increase in retrogression and runout (Zhang et al. 2018). It can also be said that highly brittle soils are more susceptible to progressive failure. Brittleness of soil is generally quantified by the brittleness index (I_B) defined as (Bishop 1971)

$$I_B = \frac{s_{up} - s_{ur}}{s_{up}} \tag{20}$$

If retrogressive failure initiates, increased brittleness of the soil changes the failure type from spread to flow slide (Wang et al. 2022). Displacement at remolded shear strength (δ_r) also controls the post-failure behavior (Dey et al. 2015; Islam et al. 2019). Dey et al. (2015) reported that an increase of δ_r changes the failure pattern from spread to flow slide. Increased δ_r results in an increase in remolding energy (area under the stress–strain curve up to remolded shear strength and strain) as well as a decrease in softening modulus. Simulation results show that increased remolding energy decreases the retrogression (Islam et al. 2018) and increased softening modulus increases the retrogression (Locat et al. 2013; Wang et al. 2016a, b); that is, a higher δ_r will result in lower retrogression (Dey et al. 2016a).

Wang et al. (2022) assessed the effect of stability number (N_s) on the occurrence of retrogressive failure and suggested that retrogressive failure doesn't occur for $N_s = 3.8$ but occurs for $N_s = 4.9$ and 6.8. They concluded that sites characterized by a low stability number are less prone to large retrogression than sites with a high stability number. Earth pressure at rest (K_{oi}) also affects the extent of retrogression. Slopes with higher K_{oi} are susceptible to large progressive spreads rather than flow slides (Locat et al. 2013; Wang et al. 2022).

The viscosity of remolded clay also affects the post-failure behavior. An increase in viscosity leads to a decrease in both the runout distance and the retrogression distance of a retrogressive failure because highly viscous fluid would consume more energy to flow (Yuan et al. 2020; Zhang et al. 2018, 2017). Zhang et al. (2018) reported that the effect of viscosity is more significant for the soils with higher sensitivity and low remolded strength. Their simulation demonstrated that the unaccounted viscosity overestimates the runout distance by 35% and the retrogression distance by 20%. Mobility of the liquified debris also affects the failure mechanism. If the liquified debris moves out of the crater easily once the retrogression has started, a flow slide is more likely to occur; on the contrary, if the liquified debris has slower movement, the failure may result in spread (Wang et al. 2022).

Tran and Solwaski (2019) demonstrated that overlooking the impact of strain rate on shear strength may overestimate the retrogression distance. Wang et al. (2022) provided further clarity on this topic, explaining the effect of strain rate during failure with respect to the reference strain rate in the constitutive model. They concluded if the strain rate at the time of failure exceeds the reference strain rate, it may overestimate the post-failure movement. Conversely, if the strain rate is lower than the reference strain rate, it may underestimate of the final retrogression and runout distance.

Wang et al. (2016a) illustrated the effect of spatial variability of undrained peak and remolded shear strength on the retrogression distance and showed that spatial variability alters the distance of retrogression. He concluded that heterogeneity significantly affects the initiation and failure mechanism, and a deterministic analysis may result in erroneous outcomes.

Effect of field conditions on the occurrence and post-failure behavior

The impact of field conditions on landslides is not straightforward and is often very complex. Landslides will respond to the combined effect of several hydrological and hydrogeological parameters (Cloutier et al. 2016). Therefore, establishing a direct correlation between specific parameters and landslide occurrence is challenging and difficult to incorporate into the numerical analysis. Hence, studies on this issue are scarce and highlight the need for more research. Wang et al. 2021) simulated the steady-state seepage condition with his strain rate-dependent strain softening constitutive soil model (Eq. 4). Pore water pressure and seepage forces are

calculated using a thermal–hydraulic analogy to model the in-situ stress condition for retrogressive failure in sensitive clay slopes. They concluded that seepage significantly influences landslide triggers. An elevated artesian pore pressure close to the slope's toe may initiate substantial failure. A rise in the earth pressure coefficient, coupled with an increase in shear strength, can alter the failure pattern from flow slide to spread and thus affect the retrogression distance.

Final discussion

In this study, the distinct characteristics of sensitive clay landslides and the advancement for modeling those landslides have been discussed in detail, focusing on the landslide types, constitutive models, numerical frameworks, and critical factors controlling landslides mechanism. It is observed that, the unique mechanism of sensitive clay landslides, i.e., its progressive or retrogressive nature is completely attributed to the strain softening nature of the soil. Whether the failure advances as successive rotational flowslide or a translational movement resulting in spread or a combination of both, it is always a result of the movement of the liquified clay. Therefore, the most essential component for the modeling of sensitive clay slopes is the constitutive soil model, which reproduces realistic strain-softening characteristics for accurately capturing the complex landslide mechanism in sensitive clays. Though several numerical frameworks are well-suited to capture the large deformation associated with retrogressive failure, the constitutive models need much improvement to represent the accurate post-failure behavior of sensitive clays. The different numerical models concerning sensitive clay landslides have been compiled in Table 1. The table presents a list of literatures on the numerical modeling of sensitive clay landslides with the constitutive model and numerical framework used, the type of landslide that has been modeled, and the outcomes of each study to give a general idea about the recent advancement and challenges in simulating landslides in sensitive clays.

Based on the review of the existing works on the numerical modeling of sensitive clay landslides, some areas that require further study are noted below.

- The most advanced constitutive model discussed in Sect. 4.1 is by Wang et al. (2022), which considered the strain rate effects, including the rheological property of soil, non-linear strength degradation, and variation of effective stress with depth. The accuracy of this model vastly depends on the large-deformation parameter, displacement at 95% strength degradation δ_{95}. A physical method to determine this parameter on the field or laboratory scale is required.
- Constitutive models used in the literature to account for sensitive clay behavior are formulated in a total stress framework which is more relevant to accounting for undrained shear strength behavior. The development of advanced effective-stress-based constitutive models is essential to evaluate in a unified coupled hydro-mechanical numerical framework long-term triggering factors with short-term rapid post-failure runouts without the need to predefine the change in calculation mode from drained to undrained analysis.
- Most of the research has been focused on landslides initiated by toe erosion, whereas research simulation related to seismic loading and other triggering factors is scanty. The influence of different field and weather conditions on failure initiation and post-failure behavior is still largely unknown and warrants further studies.
- All the numerical studies of sensitive clay landslides have been done in plane-strain conditions. Still, in reality, spatial variability in soil parameters could affect the failure mechanism to a great extent. Further investigation of 3D effects is required.
- There is scope for implementing advanced constitutive models and geometries in large deformation numerical frameworks. These tools need to be further exploited in sensitive clay landslides. For instance, constitutive models with thermo-hydro-mechanical formulations can assess the thermal effects on the creep behavior of sensitive clays (Li et al. 2018) and the mobility of retrogressive rock failures (Pinyol et al. 2018). It is essential to evaluate whether these models also apply to sensitive clay landslides.
- A limited amount of work has been performed to evaluate the effect of geometrical and material parameters for the prediction of different types of retrogressive/progressive failures in sensitive clays. Further understanding of the critical parameters is essential for landslide prediction and risk assessment of such events.

Conclusion

This study presents an elaborate review of failure mechanisms, constitutive soil models, and numerical frameworks for the simulation of sensitive clay landslides. Additionally, the results from numerical studies have been compiled in a summary table. It has been found that modeling landslides with sensitive clays is

Table 1 Summary of recent studies for numerical modeling of sensitive clay landslides

Name of the researcher	Constitutive model with strain softening	Numerical framework for large deformation	Type of sensitive clay landslide	Triggering factor	Contribution on prediction of landslides	Limitations
1. Locat et al. (2013)	NGI-ANISOFT constitutive soil model with linear strain-softening	BIFURC	Spread	Erosion	• Steeper slopes with high K_{oi}, slope with low stiffness, low remolded shear strength, high rate of strain-softening are more susceptible to large progressive failure • Spread occurs in highly over-consolidated clays	• Linear strain-softening • Strain rate effect and depth-wise variation of shear strength not considered • Rheological property of remolded clay not considered • Homogeneous slope • No demonstration for dislocation of soil mass or formation of horst and grabens
2. Dey et al. (2015)	Von-mises with exponential strain-softening	Coupled Eulerian–Lagrangian	Spread	Erosion	• Illustration for the formation of horst and grabens • Steeper slope, higher sensitivity, lower δ_{ld} are more likely to cause large progressive failure • Increase in δ_{ld}, S_t, H_{St}, and decrease in s_u of the crust changes the failure pattern from spread to flow slide	• Strain rate effect and depth-wise variation of shear strength not considered • Rheological property of remolded clay not considered
3. Dey et al. (2016a, b)			Combined	Erosion + surcharge load	• Instantaneous velocity and surcharge load accelerate the propagation of the shear band, causing progressive failure	
4. Wang et al. (2016b, 2016a)	Von-mises with linear strain-softening	Implicit & Random material point method	Retrogressive	Gravity load	• Failure surface forms in the weakest soil layer • Shear band propagation is governed by residual strength • For $S_t = 5$ the failure is translational forming horst and grabens • Spatial variability alters landslide initiation and propagation	• Linear strain-softening • Strain rate effect and depth-wise variation of shear strength not considered • Rheological property of remolded clay not considered • Homogenous slope • No clarification on the failure mechanism concerning failure type

Table 1 (continued)

Name of the researcher	Constitutive model with strain softening	Numerical framework for large deformation	Type of sensitive clay landslide	Triggering factor	Contribution on prediction of landslides	Limitations
5. Zhang et al. (2018), Zhang et al. (2020, 2017)	Bingham-Tresca with linear strain-softening	Particle finite element method	Flow slide	Erosion	• Illustration for the multiple rotational slides • Ignoring the viscosity of the remolded clay overestimates the retrogression and runout • Minimum sensitivity is required to initiate flow slide • Higher sensitivity increases the retrogression and runout • Effect of viscosity is higher for highly sensitive clays • Flow slides can result in horst and grabens	• Linear strain-softening • Depth-wise variation of shear strength not considered • Homogeneous slope
6. Tran and Solowski (2019)	Tresca with exponential strain-softening with strain rate effect	Material point method	Spread	Erosion	• Sensitive clay slope with $S_t > 25$ and $\tau_{ld} < 2$ kPa are susceptible to large progressive failure • Strain rate has a significant impact on the propagation of progressive failure	• Rheological property of remolded clay not considered
7. Islam et al. (2019)	Tresca with exponential strain-softening	Coupled Eulerian–Lagrangian	Flow slide	Seismic loading	• Steeper and inclined slopes have increased retrogression and runout • Upslope surcharge load increases retrogression and runout • Increased thickness of highly sensitive clay changes the failure pattern from spread to flow slide • Increased remolding energy decreases retrogression • A combination of rotational flow slide and translational spread can be possible in a large retrogressive failure	• Strain rate effect and depth-wise variation of shear strength not considered • Rheological property of remolded clay not considered • Assumption of static stress–strain behavior of soil under dynamic loading

Table 1 (continued)

Name of the researcher	Constitutive model with strain softening	Numerical framework for large deformation	Type of sensitive clay landslide	Triggering factor	Contribution on prediction of landslides	Limitations
8. Wang et al. 2021, 2022,	Tresca with exponential strain-softening and rate effect	Coupled Eulerian–Lagrangian	Flow slide and Spread	Erosion	• The occurrence of flow slide or spread depends on the movement of liquified debris, brittleness of soil, lateral earth pressure • Lower strain rate increases the mobility of the debris leading to a large flow slide	• No conclusive relationship between remolding energy and retrogression • Increasing stability number did not result in increasing retrogression • Some estimated input parameters (δ_{95}, β, η) for the constitutive model had high uncertainty
9. Zhang et al. (2018), Yuan (2020)	Strain-softening Tresca Model	Smoothed particle finite element method (SPFEM)	Retrogressive failure	Erosion	• Suitability of SPFM for retrogressive failure • Increased softening modulus increases retrogression and runout	• Linear strain-softening • Strain rate effect on shear strength not considered • Rheological property of remolded clay not considered • Homogenous slope
10. Shan et al. 2021	Elastoviscoplastic model	Re-meshing and interpolation technique with small strain (RITSS)	Retrogressive failure leading to spread	Decreasing shear strength of soil	• Increased S_t, decreased τ_{ld}, decreased viscosity of the remolded clay and increased riverbed width increases the retrogression	• Linear strain-softening • Homogenous slope

extremely challenging, mainly due to the distinctive soil behavior. Therefore, the constitutive model is one of the most important issues when simulating these landslides. Strain localization, formation of the shear band, failure initiation, and landslide mechanism vastly depend on the stress–strain relationship of the soil. The inclusion of a well-fit complete stress–strain curve up to the point of remolding is essential for modeling sensitive clay landslides. Furthermore, precise estimation of runout distance is not possible without considering the rheological behavior of sensitive clays after remolding. Another challenging factor is its progressive nature which requires stability analysis in both drained (failure initiation) and undrained conditions (during progressive failure) in a single simulation. Moreover, the large deformation associated with the progressive failure requires a numerical framework that captures large deformation without numerical instability and computational inaccuracy.

Acknowledgements
Not applicable.

Author contributions
Idea conceptualization: A. S. and R.C. Literature review and preparation of the complete initial draft: Z. A. U. Repeated review, restructuring, re-writing, and proof-reading A.Y. All authors read and approved the final manuscript.

Funding
No sources of funding for the research reported is to be declared.

Availability of data and materials
The datasets used and/or analysed during the current study (Presented in Figs. 11, 13, 14 and 17) are available from the corresponding author on reasonable request.
Some data generated or analysed during this study are included in these published articles.
1. Locat, A., 2007. Étude d'un Étalement Latéral dans Les Argiles de L'est du Canada et de la Rupture Progressive le Cas du Glissement de Saint-Barnabé-Nord. Laval University, Laval. https://corpus.ulaval.ca/bitstreams/0eaae92d-b076-47fe-b92e-8d6ca64142e1/download.
2. Locat, A., Jostad, H.P., Leroueil, S., 2013. Numerical modeling of progressive failure and its implications for spreads in sensitive clays. Canadian Geotechnical Journal 50, 961–978. https://doi.org/10.1139/cgj-2012-0390.
3. Locat, A., Leroueil, S., Fortin, A., Demers, D., Jostad, H.P., 2015. The 1994 landslide at Sainte-Monique, Quebec: Geotechnical investigation and application of progressive failure analysis. Canadian Geotechnical Journal 52, 490–504. https://doi.org/10.1139/cgj-2013-0344.
4. Locat, A., Locat, P., Demers, D., Leroueil, S., Robitaille, D., Lefebvre, G., 2017. The saint-jude landslide of 10 May 2010, Quebec, Canada: Investigation and characterization of the landslide and its failure mechanism. Canadian Geotechnical Journal 54, 1357–1374. https://doi.org/10.1139/cgj-2017-0085.
5. Zhang, X., Wang, L., Krabbenhoft, K., Tinti, S., 2020. A case study and implication: particle finite element modelling of the 2010 Saint-Jude sensitive clay landslide. Landslides 17, 1117–1127. https://doi.org/10.1007/s10346-019-01330-4.
6. Tran, Q.A., Sołowski, W., 2019. Generalized Interpolation Material Point Method modelling of large deformation problems including strain-rate effects—Application to penetration and progressive failure problems. Comput Geotech 106, 249–265. https://doi.org/10.1016/j.compgeo.2018.10.020.

Declarations

Competing interests
The authors declare no competing interests.

Received: 25 December 2022 Accepted: 8 May 2023
Published online: 26 May 2023

References

Augarde CE, Lee SJ, Loukidis D (2021) Numerical modelling of large deformation problems in geotechnical engineering: a state-of-the-art review. Soils Found 61:1718–1735. https://doi.org/10.1016/j.sandf.2021.08.007
Bathe K-J (1996) Finite element procedures in engineering analysis. Prentice hall, New Jersey
Bernander S (2000) Progressive landslides in long natural slopes (Licentiate thesis). Luleå University of Technology, Luleå
Bjrrum L (1955) Stability of natural slopes in quick clay. Géotechnique 5:101–119. https://doi.org/10.1680/geot.1955.5.1.101
Bjrrum L (1961) The effective shear strength parameters of sensitive clays. In: 5th International conference on soil mechanics and foundation engineering. international society for soil mechanics and geotechnical engineering, Paris
Blais-Stevens A (2019) Historical landslides in Canada resulting in fatalities (1771–2018), in: Geost. John's 2019, St. John's, Newfoundland and Labrador, Canada
Carson MA (1977) On the retrogression of landslides in sensitive muddy sediments. Can Geotech J 14:582–602. https://doi.org/10.1139/t77-059
Carson MA, Lajoie G (1981) Some constraints on the severity of landslide penetration in sensitive deposits. Geographie Physique Et Quaternaire 35:301–316. https://doi.org/10.7202/1000541ar
Cloutier C, Locat J, Greetsema M, Jacob M, Schnorbus M (2016) Potential impacts of climate change on landslides occurrence in Canada. In: Ho K, Lacasse S, Picarelli L (eds) Slope safety preparedness for impact of climate change. CRC Press, London
Crawford CB (1968) Quick clays of eastern Canada. Eng Geol 2:239–265. https://doi.org/10.1016/0013-7952(68)90002-1
Deglo De Besses B, Magnin A, Jay P (2003) Viscoplastic flow around a cylinder in an infinite medium. J Nonnewton Fluid Mech 115:27–49. https://doi.org/10.1016/S0377-0257(03)00169-1
Demers D, Robitaille D, Locat P, Potvin J (2014) Inventory of large landslides in sensitive clay in the province of Québec, Canada: Preliminary analysis. In: Advances in natural and technological hazards research. Springer Netherlands, pp 77–89. https://doi.org/10.1007/978-94-007-7079-9_7
Dey R, Hawlader B, Phillips R, Soga K (2013) Progressive failure of slopes with sensitive clay layers. In: Proceedings of the 18th international conference on soil mechanics and geotechnical engineering, Paris
Dey R, Hawlader B, Phillips R, Soga K (2015) Large deformation finite-element modelling of progressive failure leading to spread in sensitive clay slopes. Geotechnique 65:657–668. https://doi.org/10.1680/geot.14.P.193
Dey R, Hawlader B, Phillips R, Soga K (2016a) Numerical modeling of combined effects of upward and downward propagation of shear bands on stability of slopes with sensitive clay. Int J Numer Anal Methods Geomech 40:2076–2099. https://doi.org/10.1002/nag.2522
Dey R, Hawlader BC, Phillips R, Soga K (2016b) Numerical modelling of submarine landslides with sensitive clay layers. Geotechnique 66:454–468. https://doi.org/10.1680/jgeot.15.P.111
Donovan JJ (1978) On the retrogression of landslides in sensitive muddy sediments: discussion. Can Geotech J 15:441–446. https://doi.org/10.1139/t78-046
Durand A (2016) Contribution à l'étude des étalements dans les argiles sensibles de la mer de Champlain (M.Sc. Thesis). Laval University, Quebec
Eden WJ, Mitchell RJ (1970) The mechanics of landslides in Leda clay. Can Geotech J 7:285–296. https://doi.org/10.1139/t70-035
Einav I, Randolph MF (2005) Combining upper bound and strain path methods for evaluating penetration resistance. Int J Numer Methods Eng 63:1991–2016. https://doi.org/10.1002/nme.1350
Enyang Z, Wang S, Wang Y (2019) Modelling strain softening of structured soils. IOP Conf Ser Earth Environ Sci 371:022090. https://doi.org/10.1088/1755-1315/371/2/022090
Evans SG, Brooks GR (1994) An earthflow in sensitive Champlain Sea sediments at Lemieux, Ontario, June 20, 1993, and its impact on the South Nation River. Can Geotech J 31:384–394. https://doi.org/10.1139/t94-046

Fern J, Rohe A, Soga K, Alonso E (eds) (2019) The material point method for geotechnical engineering. CRC Press, Boca Raton; CRC Press, Taylor & Francis Group. https://doi.org/10.1201/9780429028090
Graham J, Crooks JHA, Bell AL (1983) Time effects on the stress-strain behaviour of natural soft clays. Géotechnique 33:327–340. https://doi.org/10.1680/geot.1983.33.3.327
Grondin G, Demers D (1996) The Saint-Liguori flakeslide: characterisation and remedial works. In: Proceedings of the 7th international symposium on landslides. Trondheim, pp 743–748
Gylland AS, Jostad HP, Nordal S (2012) Failure geometry around a shear vane in sensitive clay. In: Proceedings of the 16th nordic geotechnical meeting. Copenhegen
Hillaire-Marcel L (1980) The fauna of the post glacial seas of Quebec: some palaeoecological aspects. Geographie Phys Et Quaternaire 34:3–59. https://doi.org/10.7202/1000383ar
Hungr O, Leroueil S, Picarelli L (2014) The Varnes classification of landslide types, an update. Landslides 11:167–194. https://doi.org/10.1007/s10346-013-0436-y
Hu Y, Randolph MF (1996) A practical numerical approach for large deformation problems in soil. Int J Numer Anal Meth Geomech 22:327–350. https://doi.org/10.1002/(SICI)1096-9853(199805)22:5%3C327::AID-NAG920%3E3.0.CO;2-X
Imran J, Harff P, Parker G (2001) A numerical model of submarine debris flow with graphical user interface. Comput Geosci 27:717–729. https://doi.org/10.1016/S0098-3004(00)00124-2
Islam N, Hawlader B, Wang C, Soga K (2019) Large-deformation finite-element modelling of earthquake-induced landslides considering strain-softening behaviour of sensitive clay. Can Geotech J 56:1003–1018. https://doi.org/10.1139/cgj-2018-0250
Jin Y-F, Yin Z-Y, Yuan W-H (2020) Simulating retrogressive slope failure using two different smoothed particle finite element methods: a comparative study. Eng Geol 279:105870. https://doi.org/10.1016/j.enggeo.2020.105870
Jin Y-F, Yin Z-Y, Li J, Dai J-G (2021) A novel implicit coupled hydro-mechanical SPFEM approach for modelling of delayed failure of cut slope in soft sensitive clay. Comput Geotech 140:104474. https://doi.org/10.1016/j.compgeo.2021.104474
Karlsrud K, Aas G, Gregersen O (1984) Can we predict landslide hazards in soft sensitive clays? Summary of Norwegian practice and experiences. In: Proceedings of the 4th international symposium on landslides. University of Toronto Press, Torronto, pp 107–130
Karrow PF (1972) Earthflows in the Grondines and Trois Rivieres Areas, Quebec. Can J Earth Sci 9:561–573. https://doi.org/10.1139/e72-045
Lebuis J, Rissman P (1979) Earthflows in the Quebec and Shawnigan areas. Advances in Natural and Technological Hazards Research. Springer Netherlands, Quebec. https://doi.org/10.1007/978-94-007-7079-9_9
Lebuis J, Robert JM, Rissman P (1983) Regional mapping of landslide hazard in Quebec. In: Proceedings of the symposium on slopes on soft clays. Swedish Geotechnical Institute, Report No. 17. pp 205–262
Lefebvre G (1981) Fourth Canadian geotechnical colloquium: strength and slope stability in Canadian soft clay deposits. Can Geotech J 18:420–442. https://doi.org/10.1139/t81-047
Lefebvre G (1986) Slope instability and valley formation in Canadian soft clay deposits. Can Geotech J 23:261–270. https://doi.org/10.1139/t86-039
Lefebvre G (1996) Soft sensitive clays, Landslides: investigation and mitigation, Special report 247, Transportation Research Board. National Academy Press, Washington, DC, pp 607–619. Washington, DC
Lefebvre G (2017) Sensitive clays of Eastern Canada: from geology to slope stability, landslides in sensitive clays. Adv Nat Technol Hazards Res 46:15-33
Lefebvre G, Leboeuf D (1987) Rate effects and cyclic loading of sensitive clays. J Geotech Eng 113:476–489. https://doi.org/10.1061/(ASCE)0733-9410(1987)113:5(476)
Leroueil S, Kabbaj M, Tavenas F, Bouchard R (1985) Stress–strain–strain rate relation for the compressibility of sensitive natural clays. Géotechnique 35:159–180. https://doi.org/10.1680/geot.1985.35.2.159
Leroueil S, Ouehb L, Robitaille D, Demers D, Locat J (2011) The Saint-Liguori case history. In Understanding landslides through case studies. Subchapter 11.1. Taylor & Francis
Liu Z, L'Heureux JS, Glimsdal S, Lacasse S (2021) Modelling of mobility of Rissa landslide and following tsunami. Comput Geotech 140. https://doi.org/10.1016/j.compgeo.2021.104388
Li Y, Dijkstra J, Karstunen M (2018) Thermomechanical creep in sensitive clays. J Geotech Geoenviron Eng 144. https://doi.org/10.1061/(ASCE)GT.1943-5606.0001965
Locat A (2007) Étude d'un Étalement Latéral dans Les Argiles de L'est du Canada et de la Rupture Progressive le Cas du Glissement de Saint-Barnabé-Nord. Laval University, Laval
Locat A, Leroueil S, Bernander S, Demers D, Locat J, Ouehb L (2008) Study of a lateral spread faiulre in an eastern Canada clay deposit in relation with progressive failure: the Saint-Barnabé-Nord slide. In: Proceedings of the 4th Canadian Conference on Geohazards: from causes to management, Québec, Que., 20–24 May
Locat A, Leroueil S, Bernander S, Demers D, Jostad HP, Ouehb L (2011) Progressive failures in eastern canadian and scandinavian sensitive clays. Can Geotech J 48:1696–1712. https://doi.org/10.1139/t11-059
Locat A, Jostad HP, Leroueil S (2013) Numerical modeling of progressive failure and its implications for spreads in sensitive clays. Can Geotech J 50:961–978. https://doi.org/10.1139/cgj-2012-0390
Locat A, Leroueil S, Fortin A, Demers D, Jostad HP (2015) The 1994 landslide at Sainte-Monique, Quebec: Geotechnical investigation and application of progressive failure analysis. Can Geotech J 52:490–504. https://doi.org/10.1139/cgj-2013-0344
Locat A, Locat P, Demers D, Leroueil S, Robitaille D, Lefebvre G (2017) The saint-jude landslide of 10 May 2010, Quebec, Canada: Investigation and characterization of the landslide and its failure mechanism. Can Geotech J 54:1357–1374. https://doi.org/10.1139/cgj-2017-0085
Lo KY, Lee CF (1973) Stress analysis and slope stability in strain-softening materials. Géotechnique 23:1–11
Mitchell RJ, Markell AR (1974) Flowsliding in sensitive soils. Can Geotech J 11:11–31
Mohammadi S, Taiebat HA (2013) A large deformation analysis for the assessment of failure induced deformations of slopes in strain softening materials. Comput Geotech 49:279–288. https://doi.org/10.1016/j.compgeo.2012.08.006
Mollard JD, Hughes GT (1973) Earthflows in the Grondines and Trois Rivikres Areas, Quebec: discussion. Can Geotech J 10:324–326. https://doi.org/10.1139/e73-029
Norweigian Geotechnical Socieity (1974) Retlingslinjer for Presentasjon av Geotekniske Unders ö kelser
Norsk Geoteknisk Fbrening (1974) Retiiingslinjer for Presentasjon av Geotekniske Undersokelser. Oslo, 16 pp
NRCan, 2019. NRCan 2019 [WWW Document]. https://www.nrcan.gc.ca/science-and-data/science-and-research/natural-hazards/landslides/10661. Accessed 7 Oct 22
Odenstad S (1951) The landslide in Skoptrop on the Lidan river. In: Royal Swedish Geotechnical Institute Proceedings No. 4
Okamoto T, Larsen JO, Matsuura S, Asano S, Takeuchi Y, Grande L (2004) Displacement properties of landslide masses at the initiation of failure in quick clay deposits and the effects of meteorological and hydrological factors. Eng Geol 72(3–4):233–251. https://doi.org/10.1016/j.enggeo.2003.09.004
Pinyol NM, Alvarado M, Alonso EE, Zabala F (2018) Thermal effects in landslide mobility. Géotechnique 68:528–545. https://doi.org/10.1680/jgeot.17.P.054
Prime N, Dufour F, Darve F (2014) Solid-fluid transition modelling in geomaterials and application to a mudflow interacting with an obstacle. Int J Numer Anal Methods Geomech 38:1341–1361. https://doi.org/10.1002/nag.2260
Pusch R (1966) Recent quick-clay studies, an introduction. Eng Geol 1:413–414. https://doi.org/10.1016/0013-7952(66)90017-2
Puzrin AM, Germanovich LN (2005) The growth of shear bands in the catastrophic failure of soils. Proc Royal Soc A: Math Phys Eng Sci 461(2056):1199–1228
Qiu G, Henke S, Grabe J (2011) Application of a Coupled Eulerian-Lagrangian approach on geomechanical problems involving large deformations. Comput Geotech 38:30–39. https://doi.org/10.1016/j.compgeo.2010.09.002
Quigley RM (1980) Geology, mineralogy, and geochemistry of Canadian soft soils: a geotechnical perspective. Can Geotech J 17:261–285
Quinn P, Diederichs MS, Hutchinson DJ, Rowe RK (2007) An exploration of the mechanics of retrogressive landslides in sensitive clay. In: 60th Canadian

geotechnical conference and 8th Joint CGS/IAH-CNC groundwater conference, Ottawa, Ontario, Canada, October 21–24
Quinn PE, Diederichs MS, Rowe RK, Hutchinson DJ (2011) A new model for large landslides in sensitive clay using a fracture mechanics approach. Can Geotech J 48:1151–1162. https://doi.org/10.1139/t11-025
Quinn PE, Diederichs MS, Rowe RK, Hutchinson DJ (2012) Development of progressive failure in sensitive clay slopes. Can Geotech J 49:782–795. https://doi.org/10.1139/T2012-034
Rødvand LA, Jostad HP, Grimstad G, Andresen L (2022) Strain localisation in sensitive clays: can rate dependency provide mesh independent results? Comput Geotech 145:104678. https://doi.org/10.1016/j.compgeo.2022.104678
Rosenqvist IT (1953) Considerations on the sensitivity of norwegian quick-clays. Géotechnique 3:195–200
Rosenqvist ITh (1966) Norwegian research into the properties of quick clay: a review. Eng Geol 1:445–450. https://doi.org/10.1016/0013-7952(66)90020-2
Shan Z, Zhang W, Wang D, Wang L (2021) Numerical investigations of retrogressive failure in sensitive clays: revisiting 1994 Sainte-Monique slide, Quebec. Landslides 18:1327–1336. https://doi.org/10.1007/s10346-020-01567-4
Singh V, Stanier S, Bienen B, Randolph MF (2021) Modelling the behaviour of sensitive clays experiencing large deformations using non-local regularisation techniques. Comput Geotech 133:104025. https://doi.org/10.1016/j.compgeo.2021.104025
Skempton AW (1964) Long-term stability of clay slopes. Géotechnique 14:77–102
Skempton AW, Northey RD (1952) The sensitivity of clays. Géotechnique 3:30–52. https://doi.org/10.1680/geot.1952.3.1.30
Soga K, Alonso E, Yerro A, Kumar K, Bandara S (2016) Trends in large-deformation analysis of landslide mass movements with particular emphasis on the material point method. Geotechnique 66:248–273. https://doi.org/10.1680/jgeot.15.LM.005
Stark TD, Contreras IA (1996) Constant volume ring shear apparatus. Geotech Test J 19(1):3–11
Stark TD, Eid HT (1994) Drained residual strength of cohesive soils. J Geotech Eng 120:856–871. https://doi.org/10.1061/(ASCE)0733-9410(1994)120:5(856)
Sulsky D, Chenb Z, Schreyer HL (1994) A particle method for history-dependent materials. Comput Methods Appl Mech Eng 118:179–196. https://doi.org/10.1016/0045-7825(94)90112-0
Tavenas F (1984) Landslides in Canadian sensitive clays: a state-of-the-art. In: Proceedings of the 4th international symposium on landslides. University of Toronto Press, Torronto, pp 141–153
Tavenas F, Flon P, Leroueil S, Lebuis J (1983) Remolding energy and risk of retrogression in sensitive clays. In: Proceedings of the symposium on slopes on soft clays
Thakur V (2011) Numerically observed shear bands in soft sensitive clays. Geomech Geoeng 6:131–146. https://doi.org/10.1080/17486025.2010.546434
Thakur V (2007) Strain localization in sensitive soft clays (Doctoral Thesis). Norwegian University of Science and Technology, Trondheim
Thakur V, Degago SA (2012) Quickness of sensitive clays. Geotech Lett 2:87–95. https://doi.org/10.1680/geolett.12.0008
Thakur V, Nordal S, Grimstad G (2006) Phenomenological issues related to strain localization in sensitive clays. Geotech Geol Eng 24:1729–1747. https://doi.org/10.1007/s10706-005-5818-z
Thakur V, Jostad HP, Kornbrekke HA, Degago SA (2014) How well do we understand the undrained strain softening response in soft sensitive clays? In: Advances in natural and technological hazards research. Springer, Netherlands, pp 291–303. https://doi.org/10.1007/978-94-007-7079-9_23
Tian Y, Cassidy MJ, Randolph MF, Wang D, Gaudin C (2014) A simple implementation of RITSS and its application in large deformation analysis. Comput Geotech 56:160–167. https://doi.org/10.1016/j.compgeo.2013.12.001
Torrance JK (1983) Towards a general model of quick clay development. Sedimentology 30:547–555
Tran QA, Sołowski W (2019) Generalized Interpolation Material Point Method modelling of large deformation problems including strain-rate effects: application to penetration and progressive failure problems. Comput Geotech 106:249–265. https://doi.org/10.1016/j.compgeo.2018.10.020
Turmel D, Locat J (2018) Propagation of sensitive clay flowslides: a new approach Second JTC1 Workshop 3–5 December 2018, Hong Kong Triggering and Propagation of Rapid Flow-like Landslides
Turmel D, Locat P, Locat J, Locat A, Leroueil S (2020) The energy reduction factor (FER) to model sensitive clay flowslides using in situ geotechnical and rheological data. Landslides 17:839–853. https://doi.org/10.1007/s10346-019-01321-5
Ullah SN, Hou LF, Satchithananthan U, Chen Z, Gu H (2018) A 3D RITSS approach for total stress and coupled-flow large deformation problems using ABAQUS. Comput Geotech 99:203–215. https://doi.org/10.1016/j.compgeo.2018.01.018
Urmi ZA, Chavali RVP, Saeidi A, Yerro A (2022) Analytical and numerical assessment of the effect of erosion in sensitive clay landslide: a case study of Saint-Jude Landslide. In: Geo Calgary 2022. Calgary
Vaid YP, Robertson PK, Campanella RG (1979) Strain rate behaviour of Saint-Jean-Vianney clay. Can Geotech J 16:34–42. https://doi.org/10.1139/t79-004
Varnes DJ (1978) Slope movement types and processes. In: Schuster RL, Krizek RJ (eds) Landslides, Analysis and Control, Transportation Research Board, Special Report No. 176. National Academy of Sciences, pp 11–33.
Wang D, Bienen B, Nazem M, Tian Y, Zheng J, Pucker T, Randolph MF (2015) Large deformation finite element analyses in geotechnical engineering. Comput Geotech. https://doi.org/10.1016/j.compgeo.2014.12.005
Wang B, Hicks MA, Vardon PJ (2016a) Slope failure analysis using the random material point method. Geotech Lett 6:113–118. https://doi.org/10.1680/jgele.16.00019
Wang B, Vardon PJ, Hicks MA (2016b) Investigation of retrogressive and progressive slope failure mechanisms using the material point method. Comput Geotech 78:88–98. https://doi.org/10.1016/j.compgeo.2016.04.016
Wang C, Hawlader B, Perret D, Soga K, Chen J (2021) Modeling of initial stresses and seepage for large deformation finite-element simulation of sensitive clay landslides. J Geotech Geoenviron Eng 147:04021111. https://doi.org/10.1061/(asce)gt.1943-5606.0002626
Wang C, Hawlader B, Perret D, Soga K (2022) Effects of geometry and soil properties on type and retrogression of landslides in sensitive clays. Géotechnique 72(4):322–336
Yin Z-Y, Karstunen M, Chang CS, Koskinen M, Lojander M (2011) Modeling time-dependent behavior of soft sensitive clay. J Geotech Geoenviron Eng 137:1103–1113. https://doi.org/10.1061/(ASCE)GT.1943-5606.0000527
Yuan WH, Liu K, Zhang W, Dai B, Wang Y (2020) Dynamic modeling of large deformation slope failure using smoothed particle finite element method. Landslides 17:1591–1603. https://doi.org/10.1007/s10346-020-01375-w
Zhang W, Wang D (2020) Stability analysis of cut slope with shear band propagation along a weak layer. Comput Geotech 125. https://doi.org/10.1016/j.compgeo.2020.103676
Zhang W, Wang D, Randolph MF, Puzrin AM (2015) Catastrophic failure in planar landslides with a fully softened weak zone. Geotechnique 65:755–769. https://doi.org/10.1680/geot14.P.218
Zhang X, Sheng D, Sloan SW, Bleyer J (2017) Lagrangian modelling of large deformation induced by progressive failure of sensitive clays with elastoviscoplasticity. Int J Numer Methods Eng 112:963–989. https://doi.org/10.1002/nme.5539
Zhang W, Yuan W, Dai B (2018a) Smoothed particle finite-element method for large-deformation problems in geomechanics. Int J Geomech 18:04018010. https://doi.org/10.1061/(asce)gm.1943-5622.0001079
Zhang X, Sloan SW, Oñate E (2018b) Dynamic modelling of retrogressive landslides with emphasis on the role of clay sensitivity. Int J Numer Anal Methods Geomech 42:1806–1822. https://doi.org/10.1002/nag.2815
Zhang W, Puzrin AM, Wang D (2019) Transition from shear band propagation to global slab failure in submarine landslides. Can Geotech J 56:564–569. https://doi.org/10.1139/cgj-2017-0648
Zhang X, Wang L, Krabbenhoft K, Tinti S (2020) A case study and implication: particle finite element modelling of the 2010 Saint-Jude sensitive clay landslide. Landslides 17:1117–1127. https://doi.org/10.1007/s10346-019-01330-4

Zhou H, Randolph MF (2009) Numerical investigations into cycling of full-flow penetrometers in soft clay. Géotechnique 59:801–812. https://doi.org/10.1680/geot.7.00200
Zhu H, Randolph MF (2011) Numerical analysis of a cylinder moving through rate-dependent undrained soil. Ocean Eng 38:943–953. https://doi.org/10.1016/j.oceaneng.2010.08.005

Publisher's Note